geosciences

MDPI

Article

Modelling Individual Evacuation Decisions during Natural Disasters: A Case Study of Volcanic Crisis in Merapi, Indonesia

Jumadi [1,2,3,*], Alison J. Heppenstall [1], Nick S. Malleson [1], Steve J. Carver [1], Duncan J. Quincey [3] and Vern R. Manville [4]

1 Centre for Spatial Analysis & Policy, School of Geography, University of Leeds, Leeds LS2 9JT, UK; a.j.heppenstall@leeds.ac.uk (A.J.H.); n.s.malleson@leeds.ac.uk (N.S.M.); s.j.carver@leeds.ac.uk (S.J.C.)
2 Faculty of Geography, Universitas Muhammadiyah Surakarta, Surakarta 57162, Indonesia
3 River Basin Processes & Management, School of Geography, University of Leeds, Leeds LS2 9JT, UK; d.j.quincey@leeds.ac.uk
4 Institute of Applied Geoscience, School of Earth and Environment, University of Leeds, Leeds LS2 9JT, UK; v.r.manville@leeds.ac.uk
* Correspondence: gyjj@leeds.ac.uk or jumadi@ums.ac.id; Tel.: +44-777-834-0027

Received: 28 March 2018; Accepted: 24 May 2018; Published: 30 May 2018

Abstract: As the size of human populations increases, so does the severity of the impacts of natural disasters. This is partly because more people are now occupying areas which are susceptible to hazardous natural events, hence, evacuation is needed when such events occur. Evacuation can be the most important action to minimise the impact of any disaster, but in many cases there are always people who are reluctant to leave. This paper describes an agent-based model (ABM) of evacuation decisions, focusing on the emergence of reluctant people in times of crisis and using Merapi, Indonesia as a case study. The individual evacuation decision model is influenced by several factors formulated from a literature review and survey. We categorised the factors influencing evacuation decisions into two opposing forces, namely, the driving factors to leave (evacuate) versus those to stay, to formulate the model. The evacuation decision (to stay/leave) of an agent is based on an evaluation of the strength of these driving factors using threshold-based rules. This ABM was utilised with a synthetic population from census microdata, in which everyone is characterised by the decision rule. Three scenarios with varying parameters are examined to calibrate the model. Validations were conducted using a retrodictive approach by performing spatial and temporal comparisons between the outputs of simulation and the real data. We present the results of the simulations and discuss the outcomes to conclude with the most plausible scenario.

Keywords: agent-based model; evacuation model; evacuation decision; risk perception model; volcanic hazard; synthetic population; Merapi

1. Introduction

Geophysical events, such as earthquakes, volcanic eruptions, landslides, and flooding, have been occurring on the planet long before the advent of humans, but these events are transformed into natural disasters when they threaten human life [1]. The occurrence of natural disasters has increased over the last decades in line with the increase in the human population, because more people are now occupying those areas which are susceptible to such events [2]. While disasters occur worldwide, they have the greatest impact in developing countries due to the prevailing physical (i.e., geographic and geologic) and social conditions [1]. During the last decade, the number of affected people increased greatly in 2015 compared to the period 2005 to 2014, with the highest percentage in Asia [3]. In that

year, Indonesia was the fourth most frequently affected Asian country [4]. Among the various natural hazards, volcanic eruptions pose a significant threat to Indonesia, as it is located within the "Ring of Fire" [5]. Merapi is the most active volcano in Indonesia, and the 2010 eruption was ranked third in the world since 2005 in terms of impact [4]. Being in such susceptible areas, people living close to Merapi should, therefore, develop their awareness and preparedness to evacuate when a hazard occurs.

Evacuation is an important life-saving action in any disaster [6], with a history as old as human history in saving lives from natural disasters [7]. It takes place by moving people from a hazardous area to a safer place in a very limited time [8]. This time limit depends on the speed of the onset of the hazard. Some hazards occur rapidly, with others more slowly [1,9]. For example, hurricanes or earthquakes happen very quickly, while global temperature variations, rises in sea level, drought, and disease affect society more slowly [9]. For fast-onset hazards, immediate responses leading to evacuation are needed, because being at the wrong place at the wrong time will quickly lead to fatalities. Volcanic eruptions can happen several days after the initial signs of instability, but it is also possible for them to happen several weeks later [10]. Therefore, immediate responses from the surrounding population are needed, but there are often cases of people who refuse, or are reluctant to evacuate from hazardous areas [7]. For example, in two crises in Merapi (2006 and 2010), it was recorded that some people stayed even after official evacuation orders from the local authorities. In the 2006 eruption, individuals in some areas of Merapi disobeyed the evacuation order and suffered the consequences of the eruption [11]. Likewise, reluctance was one of the main issues in the volcanic crisis management of the 2010 eruption [12].

This phenomenon can hamper evacuation processes, but has received surprisingly little attention in studies on evacuation modelling (e.g., [13–16]). Modelling the emergence of reluctant people during a crisis might help in improving evacuation plans; that is, to what extent the number of reluctant people can be reduced to save more lives. This paper aims to model the individual decision-making processes of evacuation (evacuate/stay) during a volcanic crisis using an agent-based model (ABM). The model uses several interacting factors [17–20] that drive people to leave (forced to evacuate) versus the driving factors to stay (forced to stay). Mt. Merapi in Indonesia was used as a case study, with records from the 2010 eruption and associated documentation used as empirical data to validate the model. In the paper, Section 2 will present the background literature within this field. Section 3 presents the methodology of the research and also gives an introduction to the study area, the synthetic population generation technique, and data on past eruptions. A description of the ABM using Overview, Design concepts and Details (ODD) protocol [21,22], and the calibration and validation techniques are also included in this section. Section 4 presents the results and discussion, followed by the conclusion in Section 5.

2. Background

The decision to evacuate is not only complex, but also dynamic. Therefore, developing a model can be intricate and needs an appropriate approach. It is a complex social process, resulting from many interrelating physical and social factors. Studies have identified that evacuation decisions are influenced by several factors [23–25] including: (1) risk communication and warning; (2) perception of risk; (3) community and social network influence; and (4) disaster likelihood, environmental cues, and natural signals. As a social process, it will be dynamically changed nonlinearly as the above factors also change.

Risk communications deal with the dissemination of risk warnings regarding the probability of a disaster occurring within the community. There are three types of interaction models in emergency situations, namely vertical (top-down), peer to peer, and horizontally broadcast [26]. On the other hand, risk perception is a critical aspect of understanding how individuals decide to evacuate or to stay put [23]. Risk perception is also responsible for influencing people's decisions on when they should evacuate, and when they should return home during a crisis [27]. Perception, from the geographer's point of view, describes how things that are related to the surrounding environment are remembered and recalled by people [28], whereas risk perception is the way people interpret the likelihood of

danger, with those who believe that they are not at risk (perceive themselves as safe) tending to feel that evacuation is not essential [29]. Several factors influence risk perception, including social and cultural factors, gender, and experience [23]. Another study by Botzen et al. [30] has stated that some demographic aspects, namely location, experience, knowledge, and socioeconomic status, contribute to the perception of the population toward risk. The perceptions of people who live on and around the volcano commonly vary, and this affects the warning-response outcome [31,32]. Community and social networks also play an important role in influencing how people respond to a disaster. People tend to keep within their group (community) in their decision response in such situations [33], so they will stand together with their family when deciding to stay or to leave [34]. Moreover, in crises people are more easily influenced when they interact with a group rather than with individuals. Therefore, people may decide to leave themselves after seeing crowds of evacuees leaving their homes. Lastly, disaster likelihood, environmental cues or natural signals also affect evacuation decisions [29,35]. Some studies on volcano and flood evacuation have identified that natural signals are the most critical factor in evacuation decisions [29], while others state that risk perception is associated with environmental cues, as well as with the characteristics of the hazard [25].

These aspects should all be considered when modelling evacuation decisions in order to better understand how willingness and reluctance emerge. Several studies highlight that traditional beliefs, culture/inherited local knowledge, and economic aspects are found to be the common reasons for refusing to follow evacuation orders [19,31,36–38]. Although the economic aspect has no influence in the case of evacuation decisions in Merapi [19], it does encourage people to return home to protect their property or to feed cattle during the evacuation period [18]. Some modelling studies show how social processes affect evacuation decisions. An example of a communication model among agents within a group, and from one group to different groups, has been presented by Canessa and Riolo [39]. Agent interaction, specifically the mechanisms of how actions and messages from other agents motivate individuals, can be represented using an agent-based model [40]. The aggregation behaviour of people was successfully presented by Qiu and Hu [41]. However, models of the decision-making mechanisms as a result of these factors are limited. The evacuation decision model (EDM) developed in this paper is different from another recent model based on perceived risk by Reneke [42] and improved by Lovreglio et al. [43]. These models [42,43] disregard the social characteristics of agents in defining risk perception. However, based on other research, risk perception does not stand alone, but depends on other factors [23,30,44]. Therefore, this paper attempts to address this problem by involving risk perception and some of the other aforementioned factors in evacuation decision making. For this purpose, Agent-based modelling (ABM) was employed to simulate the decision making mechanism during an emergency situation.

ABM, which in some literature is called ABS (agent-based systems) or IBM (individual-based modelling) [45], is defined as a computational method that enables a researcher to create, analyse, and experiment with models comprising agents that interact within an environment [46,47]. These agents can be separate computer programs, or in the common form, distinct parts of a program that are used to represent social actors, which can be individual people, organisations, such as firms, or bodies, such as nation-states [46]. The agent can also be represented in a spatially realistic environment involving a Geographic Information System (GIS), which is called spatial agent-based modelling [48] or georeferenced agent-based model [49]. The conceptual integration of both GIS and ABM is achieved successfully by Brown et al. [50], where GIS is used as the spatial data model representation, and ABM as the processes model. Such a model is suitable for developing an emergency evacuation model, considering the spatial aspects of both hazard and population.

In addition to ABM, there are several other computer simulation techniques for emergency simulation and evacuation, namely system dynamics, stochastic modelling, queuing networks, lattice gas models, social force models, fluid-dynamic models, and game theoretic models [51,52]. GIS and cellular automata (CA) are also used by some models for the same purposes [53–57]. However, ABM has more benefits in modelling individuals in emergencies, including the possibility

to capture emergent phenomena, to naturally describe the system, and flexibility [51,58]. ABM and CA share some similar characteristics, but ABM is superior since CA is less able to represent the heterogeneity of agents within a population [52,59]. With particular reference to evacuation modelling, Zheng et al. [52] compared seven methodologies for simulating crowd evacuation, including CA and ABM. Their study highlighted that only simulation using ABM has the capability to model heterogeneous agents at a microscopic scale; this ability is important to model evacuation with varying population characteristics.

Although the development of ABM is intricate, such as being a complicated development process, being difficult to understand, challenging to collect the required data, difficult to validate, commonly needing very large runs due to the randomness, and complex in analysing the output, it provides a promising approach to simulating human-natural system interaction [21,60–66]. Its advantages enable ABM to be better at representing human behaviour in decision-making [67], especially when dealing with disaster events. This approach has been applied to a range of hazards; for instance, fire and building damage-related hazards [68–71], hurricanes [13], and tsunami [14,67]. These models vary in terms of the spatial extent of the simulated areas, the population mimicking method, integration of the hazard model, and the evacuation decision of agents. Fire and building damage-related hazards apply to a smaller spatial extent than hurricanes and tsunami, which use regions/cities as simulation areas.

Wider areas imply more complexity in the agent population and evacuation routes. Small area evacuation, such as in fire evacuation models, use only a small number of evacuees, making their characteristics less complex. These models commonly generate a number of agents randomly as building occupiers in the simulations (see [69,70]). More complex agent populations simulated in models should implement synthetic populations to imitate real world heterogeneity (see [72–74]). However, few of the evacuation models have used this approach in generating the population of agents. This approach might not be important for a model intended for experimental purposes only (such as [13]), but it should be applied to a model that uses real data with heterogeneous population characteristics. The emergence of a new library for synthetic population generation, such as Gen* [61], is promising for future enhancement of this aspect.

3. Materials and Methods

3.1. Study Area

Mt. Merapi (110°26.5′ E, 7°32.5′ S) in central Java is one of the most active volcanoes in Indonesia [75]. More than 1 million people live in the vicinity, with 400,000 people at especially high risk [76,77]; the city of Yogyakarta (population 4 million) lies only 28 km to the south. There is a record of dangerous eruptions going back many hundreds of years, with an average interval between eruptions of 1–6 years [10,78]. More than 74 eruptions have been recorded since 1548 AD, most of them around VEI 2 [79], but larger events (VEI > 3) occurred in 1672, 1822, 1846, 1849, 1872, 1930–1931, and 1961 [10,78,80]. Eruptions in the 20th century have caused many deaths, including those of 1930 (1400 deaths), 1954 (54 deaths), 1961 (6 deaths), and 1994 (69 deaths) [81,82], while the VEI 4 [79] eruption in 2010 was the largest in over a century, ejecting 30–60 million m^3 of pyroclastic material [83] and resulting in 332 deaths and 1705 injuries [84]. As an active volcano, further large explosive eruptions of Merapi should be anticipated by studying its characteristics from historical events [10].

The historical activity of Merapi is dominated by the episodic growth and collapse of andesitic lava domes at the summit (2978 m a.s.l. prior to the 2010 eruption). Less frequently, the summit dome complex is destroyed by more massive explosive eruptions. Lava dome collapse triggers a range of pyroclastic density currents (PDCs), a general term applied to fast-moving ground-hugging mixtures of hot gas, rock fragments, and ash, which have both dilute, turbulent (surge) and dense pyroclastic flow (PF) end-members [85]. At Merapi these include: (i) high energy dilute, turbulent pyroclastic surges; (ii) valley-confined, relatively dense block-and-ash flows (BAF), comprising juvenile volcanic

blocks in an ash matrix, sometimes referred to as Merapi-type *nués ardentes* [86,87], which travelled as far as 16.5 km during the 2010 eruption [88]; (iii) unconfined and overbank pyroclastic flows; and (iv) dilute ash cloud surges elutriated and decoupled from the denser flows [81,89].

Rain-triggered *lahars* are a serious additional hazard at Merapi, both during and after eruptions, when heavy rainfall remobilises fresh pyroclastic deposits [90]. The word *lahar* is an Indonesian term referring to a sediment-laden flow of water from a volcano, other than the normal stream flow [91]. At Merapi, lahars, including both debris- and hyper-concentrated flow types [92], can travel at 5–7 m/s at elevations above 1000 m a.s.l. and reach as far as 30–40 km from the summit along each of the several rivers that drain the mountain, inundating extensive areas of the ring plain below 600 m a.s.l. and aggrading channels [81,93–97]. In comparison with the PDC and lahar hazards, distal ashfall is a relatively minor phenomenon at Merapi [98].

Geographically, Merapi spans four regencies of two provinces, i.e., Sleman (Yogyakarta), Magelang, Boyolali, and Klaten (Central Java). This study focuses on the Sleman regency, lying on the southern flank of Merapi (Figure 1) between 107°15′03″ to 107°29′30″ E and 7°34′51″ to 7°47′30″ S. The area covers 57,482 hectares (574.82 km^2), or about 18% of the Yogyakarta metropolitan area. Administratively, the region contains 17 sub-districts, 86 villages and 1212 hamlets. The area was selected because it is located on the southwest flank of Merapi, which is prone to disaster [99], and also due to the significant geomorphic [100] and geological changes [80] produced by the 2010 eruption, which have potentially changed the likely run-out direction of the pyroclastic and lahar flows, impacting the accuracy of existing hazard maps (see Figure 1) [101,102].

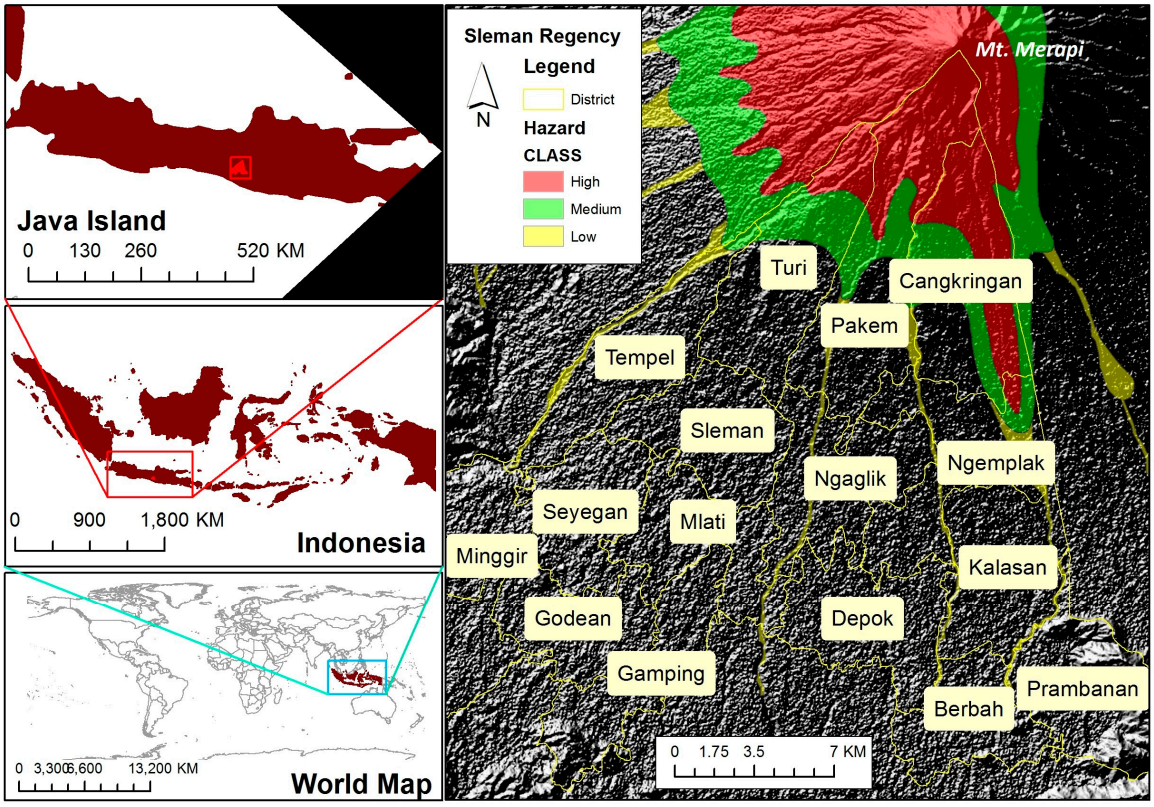

Figure 1. Study area and hazard zones.

3.2. General Framework

The framework to develop the model (Figure 2) mainly comprises preparation, model development and simulation, calibration, and validation. The purpose of the preparation step is to collect and analyse the dataset that is used to generate the variables and formulate the rules in the simulation

(see Section 3.3). The simulation step includes the development of the ABM application and experimentation based on the formulated rules. Calibration and verification steps are needed when the output of the model is unacceptable (see Section 3.6.2). The aim of the calibration was to adjust the variables used in the model, whereas verification aimed to improve/revise the rules and the ABM application. When the revision/improvement was complete, re-simulation and re-validation were then needed iteratively. Two adjustments were made to the hazard model, while the decision model was adjusted three times, resulting in three simulation scenarios. Finally, the validation step compared the simulation output of both the spatial and temporal data (see Section 3.6.3).

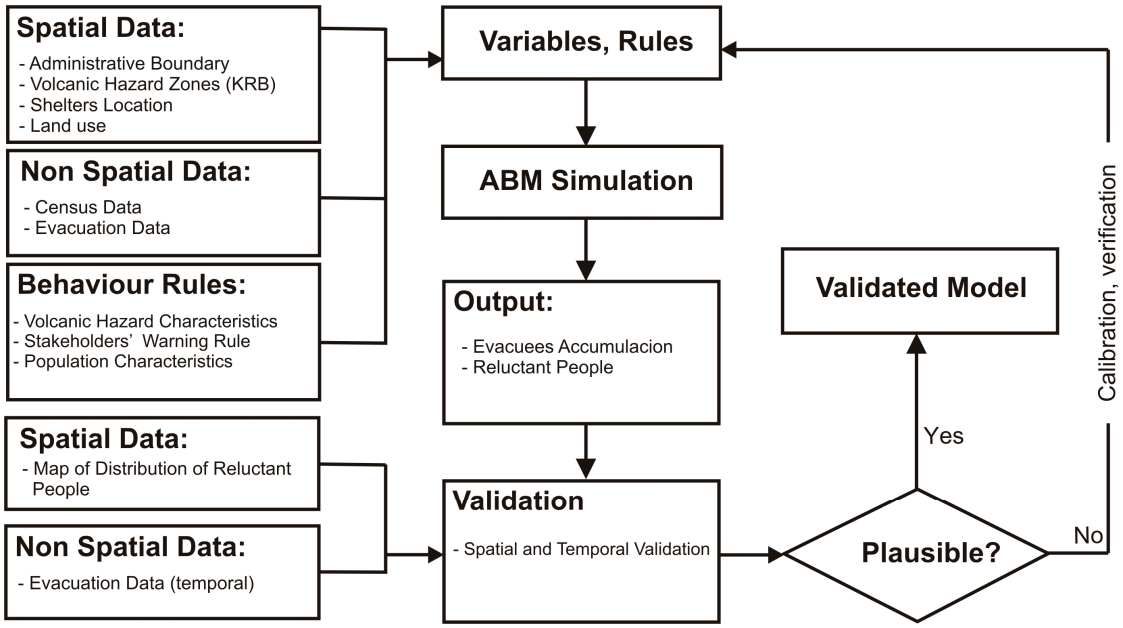

Figure 2. General framework.

3.3. Input Data

Several types of spatial and non-spatial data from Merapi were collected and used to generate the agent and environment (Table 1). The spatial data mainly comprises the administrative boundaries of Sleman, the volcanic hazard zone, land use, and road network. The non-spatial data comprises microdata from the Indonesian Census of 2010 from IPUMS [103], demography, and population characteristics developed from the survey. For the survey, we used a questionnaire to explore decision-making behaviour on the basis of households (disaggregate). The results provided a probability distribution of people most likely to evacuate for every level of volcanic activity. Five primary variables were collected from the questionnaire survey, namely socio-demographic characteristics, perception of volcanic hazard, decision-making behaviour, interaction during a crisis, and willingness to accept an alert. In order to collect these variables, stratified random sampling was applied. Household member samples, represented as building units, were selected randomly for each building block (*dusun*). This area segmentation is based on the consideration that each *dusun* has one village's chief who mobilises people (*Rukun Tangga*) and, commonly, in rural areas of Indonesia, has homogenous social characteristics. Twelve villages were selected within a radius of 20 km. We created several ring buffers with distance ranges of 5 km to define the sampling areas, with three villages selected from each range. Furthermore, 10 participants from each village were selected randomly, resulting in 120 participants in total. The results of the survey were statistically analysed to develop the evacuation decision model (see Supplementary Material—Appendix 1). These were also used to partially characterise the agents (the majority of agent characteristics were taken from census microdata).

Table 1. Dataset list for the model.

Data	Source	Use
ABM Development		
Administrative boundary	Indonesian Geospatial Agency (BIG)	This data is used to distribute the human agents within the boundary.
Volcanic hazard zones	(1) National Agency for Disaster Management (BNPB); (2) Based on the evacuation order hazard zones in 2010 [76]	Setting up the hazard scenarios and spatial distribution of the eruption impact.
Shelter location	Geospatial BNPB [104–107], DYMDIS GEGAMA [108]	Defining evacuation destination.
Land use	Indonesian Geospatial Agency (BIG)	Defining the mean centre of population distribution (synthetic population generation).
Census microdata	Microdata of the Census of Indonesia 2010 from IPUMS [103]	Defining the sociodemographic characteristic distribution (synthetic population generation).
Road networks	OSM PBF File [109]	Evacuation routing
Survey data	Survey	Formulating the decision making.
Validation		
Map of distribution of reluctant people	Evacuation refusal map [12]	Spatial validation.
Series of daily records of evacuees in 2010 eruption	Local Government of Sleman [110]	Temporal validation.

3.4. Model Design

3.4.1. Overview

Purpose

The purpose of the simulation was to model individual decisions in the volcanic evacuation which led to reluctance and to validate the output with real data. The validation is based on temporal and spatial data from the evacuation of 2010. The temporal data is the evacuation dataset (see Supplementary Material—Appendix 2) that provided in daily basis during the crisis, whereas the spatial data is the emergence of reluctant people (see Supplementary Material—Appendix 3).

Entities, State Variables, Scales, and Environment

The ABM is based on a model from Jumadi et al. [15] that mainly consists of three agent types, namely, the volcano, people, and stakeholders. Additionally, there are safe shelters, which are objects assigned as properties of the environment, together with districts, hazard zones, and routes. A detailed description of the entities and the corresponding attributes is provided in a previous article [15], with some improvements in the people agent provided in Table 2. The following is a brief description of each element:

- Volcano: this agent represents Mt. Merapi, which has the rule to produce activity and trigger a change in the environment.
- People: this agent type represents people, generated based on the census data as synthetic population agents (see Section 3.5 for details of the synthetic population generation).
- Stakeholder: this is an agent who acts as stakeholder, with the role to alert people to evacuate.
- Environment: this is represented as a spatial environment where the agents live. It consists of: (1) the population unit, which is a fixed environment provided as a GIS region; (2) the administrative boundary of the district where the agent's population will be distributed within the region; (3) hazard zones to model the hazardous environment that dynamically changes following the volcanic

activity; (4) the route networks that are used by agents to move; and (5) evacuation shelters, which are distributed outside the hazard zones as GIS points.

Table 2. Overview of main attributes additional to the previous model [15].

Entity	Attribute	Type	Description
People	Disability	Integer	Expresses whether the agent has a disability or not.
	Experience	Integer	Expresses whether the agent has experienced a previous eruption or not.
	Income	Integer	Income class of agent.
	PersonalIntension (PI)	Integer	The degree to which people are motivated to evacuate by themselves (taken from the survey).
	ProtectProperty (PP)	Integer	The degree to which are people motivated to stay to protect their property (taken from the survey).
	SeeTheExplosion (SE)	Boolean	Whether the agent has seen the volcanic eruption or not.
	Perception	Integer	This value describes how well the agent perceives the hazard.
	CulturalBelief (CB)	Integer	The degree to which people are motivated to stay by their beliefs (estimated from the literature; this is only assigned to aged and poorly educated people).
	GovernmentAlert (GA)	Integer	The degree to which people are motivated to evacuate when they receive an alert from the stakeholder (taken from the survey).
	FeelingDanger (FD)	Integer	Quantification of feeling in danger.
	FeelingSafe (FS)	Integer	Quantification of feeling safe. This will be deduced when FD increases.
	NotKnowingTheDestination (ND)	Integer	The degree to which people are motivated to stay because they do not know where to go (taken from the survey).
	TransportConcern (TC)	Integer	The degree to which people are motivated to stay because they have a problem with transportation (taken from the survey).
	SocialInfluence (SI)	Integer	The degree to which people are motivated to evacuate by their social relation decisions (taken from the survey).

Process Overview and Scheduling

The model comprises several processes: (1) volcanic activity generation; (2) the stakeholder's alerting procedures; and (3) people's individual decision-making. The volcanic activity will change over the time of the simulation. The length of crisis can be either predefined at the simulation start or randomly generated by the simulation, while the stakeholder is observing this activity during the simulation. When the activity changes, it will be analysed against the alerting rules. The alert will be sent to the population if the condition fulfils the requirements of evacuation order issuance. Otherwise, the stakeholder will continue to observe the volcano. The population can observe the volcanic activity and the environment, as well as receiving commands from the stakeholder. People will evacuate when the conditions meet the criteria. Details of the procedures are provided in Section 3.4.3.

3.4.2. Design Concepts

The following concepts will be used in the model:

- **Emergence**: by simulating the evacuation decision in a spatiotemporal dynamic model, the potential problems for evacuation may emerge, especially the emergence of reluctant people.
- **Sensing**: the stakeholder can sense the change in volcanic activity level by reading the signal (message) from the volcano. Human agents can sense their location, and whether they are located in a danger zone or not.

- **Interaction**: the stakeholder interacts with the human agents regarding the alert issuance. Human agents interact with each other to convey their decision to evacuate.
- **Stochasticity**: the socio-demographics and location of the human agents are generated randomly. The socio-demographics are generated using custom distribution based on census microdata, whereas the location of agents is generated based on the settlement distribution generated from land use data [111].
- **Observation**: the output can be monitored directly during the simulation from the map, as well as the monitoring charts. Some indicators are observed during the simulation, including the percentage of people at risk (low, medium, high), the percentage of evacuating people, occupancy of the evacuation shelters, and the level of volcanic activity. This output is also recorded as a CSV file that can be spatiotemporally analysed using GIS, or Excel for other purposes.

3.4.3. Details

Initialisation and Input

The initialisation of the model relies on the input data previously provided in Section 3.3, complemented with data from the literature and author estimation of missing data. The volcano attribute initiation values are mostly based on data from the literature. In addition, the population attributes are mostly from the statistical data derived from the census microdata and the survey. We developed a custom distribution based on these statistics to initiate the value of the demographic attributes. A custom distribution is a feature in AnyLogic 8.2 (The AnyLogic Company, Oakbrook Terrace, IL, USA), developed based on frequency from the observed samples [112]. Meanwhile, the stakeholder has simple attributes taken from the literature. The overall parameterisation of agents in the model is provided in Table 3. In this initial condition, the environment is assigned with safe or low hazard, depending on the hazard zone.

Table 3. Overview of the initialisation of the primary attributes.

Entity	Attribute	Initial Value	Unit	Changing Mechanism	Source
Volcano	Latitude	−7.541	Degree	Fixed	[102]
	Longitude	110.446	Degree	Fixed	[102]
	ActivityLength	104	Days		[76]
	ActivityLevel	0	-		[76]
	VEI	4	-	Fixed	[102]
Stakeholder	AlertLevel	1	-	Changed by changing ActivityLevel	[76]
People	Age	Based on custom probability	Years	Fixed	Dataset [103]
	Disability	Based on custom probability	-	Fixed	Dataset [103]
	Education	Based on custom probability	-	Fixed	Dataset [103]
	Experience	Based on custom probability	-	Fixed	Survey Data
	HouseHoldID	From Simulation	-	Fixed	Simulation
	Income	Based on custom probability	-	Fixed	Dataset [103]
	DistrictID	From simulation	-	Fixed	Simulation
	Sex	Based on custom probability	-	Fixed	Dataset [103]
	Latitude	From simulation	Degree	Changed by movement	Simulation
	Longitude	From simulation	Degree	Changed by movement	Simulation

Table 3. *Cont.*

	HomeLatitude	From simulation	Degree	Fixed	Simulation
	HomeLongitude	From simulation	Degree	Fixed	Simulation
	MovementSpeed	30–40	km/h	Fixed	[113]
	PersonalIntension (PI)	1–5		Fixed	
	ProtectProperty (PP)	1–5	-	Fixed	Simulation
	SeeTheExplosion (SE)	0	-	Changed by the volcano activity	Simulation
	Perception	1–5	-	Fixed	Simulation
	CulturalBelief (CB)	0–5	-	Fixed	Simulation
	GovernmentAlert (GA)	0	-	Changed when alert received	Simulation
	FeelingDanger (FD)	0	-	Changed by the volcano activity and the hazard zone	Simulation
	FeelingSafe (FS)	5	-	Changed when FD changes	Simulation
	NotKnowTheDestination (ND)	1–5	-	Fixed	Simulation
	TransportConcern (TC)	1–5	-	Fixed	Simulation
	SocialInfluence (SI)	0	-	Changed when receiving alert by social network	Simulation

Sub-Models

1. Volcanic Activity

During a period of crisis, the activity level of the volcano (VAL) changes over time. This activity can be divided into four classes: normal (out of the volcanic crisis period), low, medium, and high. For instance, the data from two crisis records (2006 and 2010) show how the relative length of each level varies randomly (see [11,114] for chronological details). Temporally, the VAL changes over time, typically from low to medium to high to medium to low. This spatially affects the changes in the hazardous environment in the model. Similarly, the variability of the Volcanic Explosivity Index (VEI) also affects the variability of the spatial extent of the impact. The impact will be much wider when the intensity is higher. VEI is a qualitative index used to describe the magnitude or the destructiveness of an eruption [79], ranging from 0 (least destructive) to 8 (most destructive) [79]. Based on historical records, the VEI of Merapi eruptions ranges from 1–4 [83]. The rule in this model on how VAL and VEI influence the hazard zone is provided in Table 4 (a more detailed illustration is provided in figure 4 of a previous paper [15]).

Table 4. Matrix relationship between the Volcanic Explosivity Index (VEI), VAL and the hazard level within hazard zones (adapted from [15]).

VEI	1			2			3			4		
Hazard Zone / VAL	L	M	H	L	M	H	L	M	H	L	M	H
III (H)	L	M	M	L	M	M	M	H	H	M	H	H
II (M)	L	M	M	L	M	M	M	M	H	M	M	H
I (L)	L	L	M	L	L	M	L	M	M	L	M	M

Notes: L: Low, M: Medium, H: High.

2. Official Warning Models

Alerts and warnings are part of the social capacity of the community in a disaster. Disaster warning is a communicative process comprising interrelated activities and procedures [115]. As this is produced

from observation of the likelihood of disaster, it is commonly included with many uncertainties and limitations that can fall to the false warning and missed event [116]. The sources of warnings can be authorities, peers, friends or family members, and media [117]. The authorities issue disaster warnings in Merapi from the observation of activity levels. Subsequently, warnings are delivered to all agents; the warning level is derived from the VAL. The warning steps, referring to the actual warning procedure in Merapi, are provided in Table 5 [76].

Table 5. Alert rules in Merapi.

VAL	Definition	Volcanic Activity	Evacuation Alert
I	Normal activity	No indication of activity change, either visual likelihood or seismicity level.	No Evacuation alert
II (Low)	On guard	Indications of activity are increasing, either from visual likelihood on the crater, or seismicity level.	No Evacuation alert
III (Medium)	Prepare	Seismic activity is increasing intensely, with obvious visual changes on the crater.	Prepare to Evacuate
IV (High)	Beware	About to erupt.	Evacuate

Adapted from Mei et al. [76].

3. Evacuation Decision Model of People

The human agents in the ABM are utilised with the ability to decide to evacuate or to stay, based on the threshold rule [118,119] and evacuation states model of Lovreglio et al. [43]. The decision is made by evaluating social and physical factor variables (Figure 3). These factors are quantified, weighted, and classified into two main categories: driving factors to evacuate (EF) or driving factors to stay (SF) (Figure 3a). A detailed description and quantification of EF and SF are provided in the supplementary material (Appendices 4–6), where the weight of the factors varies based on the scenario setting (see Section 3.6.2). Both EF and SF are used in Equation (1) to define the strength of the evacuation decision (ED). Agents use threshold-based rules [118,119] to evaluate the ED (Figure 3b). The change in ED triggers the transition between the states of Normal-Investigating-Evacuating. When the agents have enough EF, i.e., they exceed the threshold, they will evacuate, otherwise they will continue to stay. An overview of the states is provided as follows (a detailed state chart diagram is provided in the Supplementary Material—Appendix 7):

- Normal: initial state of agent when there is no sign of hazard.
- Investigating: the agent observes the volcano and their environment (social, physical) as the activity of the volcano increases.
- Evacuating: the agent decides to evacuate. In this state, the agent warns their family as well as their relations to evacuate.

$$ED = EF - SF \quad (1)$$

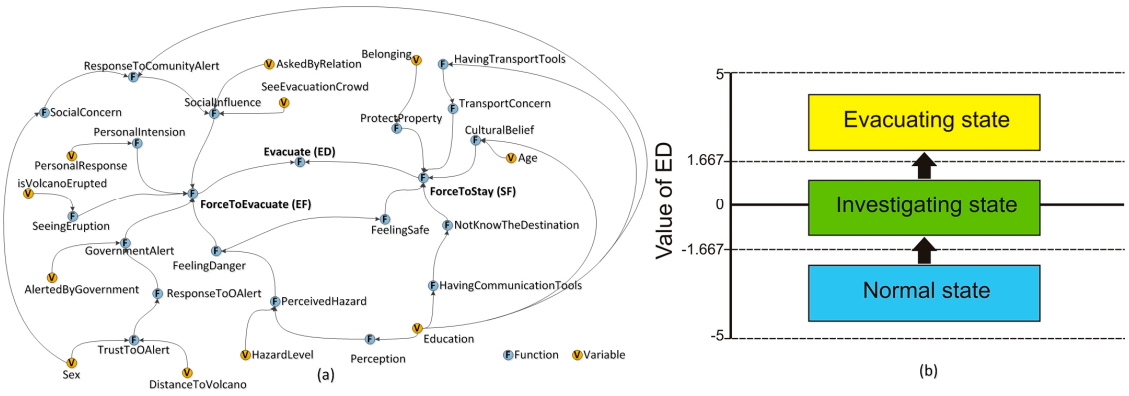

Figure 3. Threshold-based decision rule based on the Normal-Investigating-Evacuating state model. (**a**) The interrelating variables and functions define the value of the evacuation decision (ED); and (**b**) the transition between states in the evacuation decision as result of changing ED based on the threshold model. Descriptions of the variables and functions are provided in the supplementary materials (Supplementary Material—Appendices 5–7).

3.5. Population and Synthetic Population Generation

Spatially realistic ABM requires the utilisation of realistic agent attributes and localisation (spatial distribution) [61]. However, population microdata is commonly lacking in spatial representation details of household location due to confidentiality issues [120]. Moreover, the aggregate characteristics of human agents need to be consistent with the aggregate characteristics of the real population [121]. This population characteristic should be similar to the real situation regarding socio-demographic attributes as well as spatial distribution [122]. Therefore, the synthetic population generation characterizes not only the demographic character, but also the geographic location, to fulfil this requirement.

The synthetic population is a population built from anonymous survey data at the individual level [122]. In this model, the individuals will be grouped into households to represent reality. There are several techniques to generate a synthetic population, including deterministic reweighting, conditional probability (Monte Carlo simulation) and simulated annealing [123]. Among these techniques, conditional probability has advantages for use in this model as it contains stochastic elements. This stochastic condition is needed because the exact location is unknown. The general technique for generating the synthetic population in this model is provided in Figure 4. The technique comprises three steps: data preparation; conditional probability simulation development and execution; and verification to fit the result. Development, execution, and verification are iterative processes. If the verification finds high deviation between the real data, it then loops back to the development and execution process to fix possible bugs or logical errors.

The details of the Monte Carlo simulation to generate the synthetic population model are based on a method by Moeckel et al. [124]. In this model, human agents are generated for each sub-district of Sleman in individual units grouped as households. The attributes are matched with the real data using census data statistics and field data from questionnaires. The spatial distribution of the population is also randomly generated to be matched with the real spatial distribution of the population using the centre of gravity model [111]. Due to software and computer resource limitations, the simulated population was minimised proportionally (Table 6).

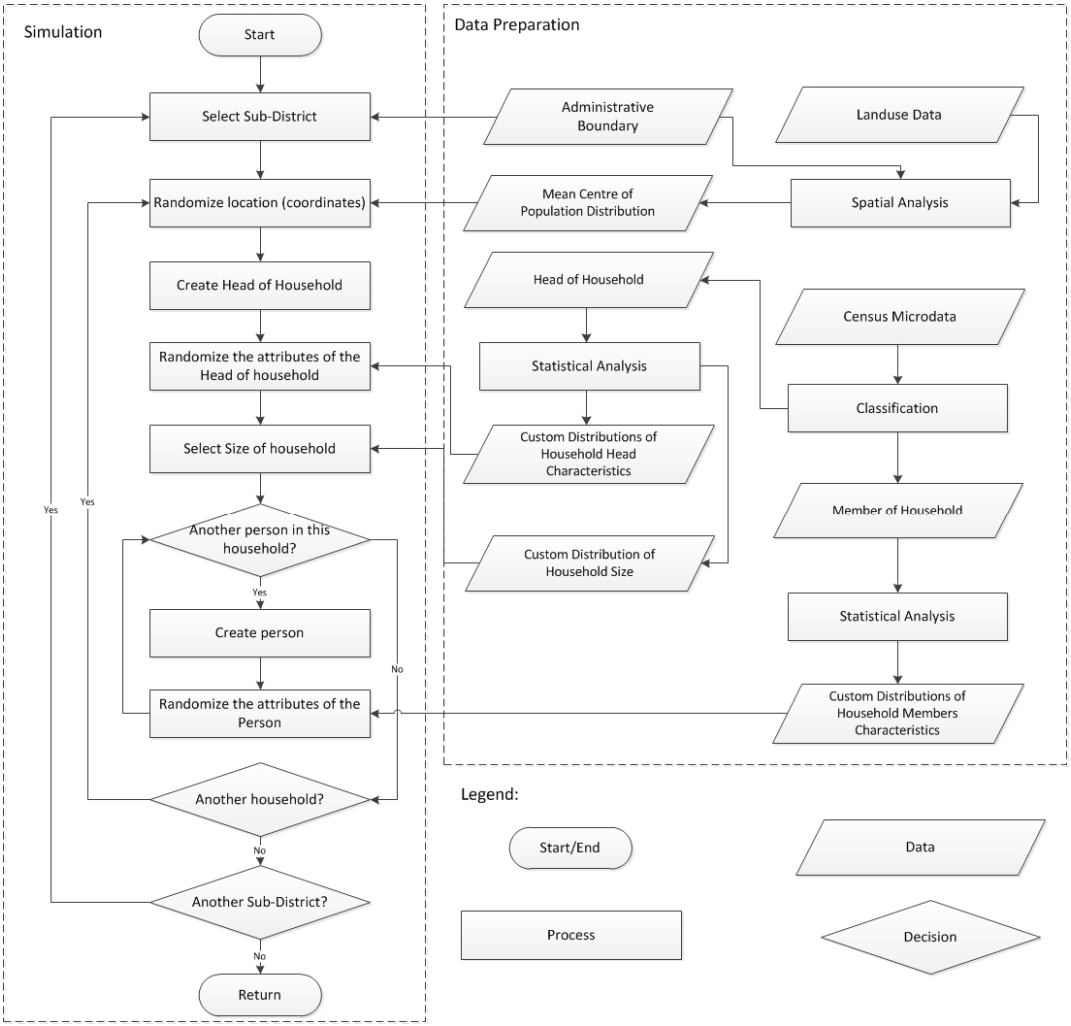

Figure 4. Synthetic population generation.

Table 6. Real population level (2010) and simulated agents.

District	Population Mean Centre		Number of Households	Number of Simulated Households	Estimated Level of Simulated Population
	Longitude	Latitude			
Berbah	110.448997	−7.802559	18,927	473	1892
Cangkringan	110.456001	−7.649149	9187	230	920
Depok	110.400001	−7.773849	47,228	1181	4724
Gamping	110.334999	−7.78209	31,724	793	3172
Godean	110.301002	−7.77015	24,619	615	2460
Kalasan	110.467002	−7.74484	25,277	632	2528
Minggir	110.238998	−7.73681	13,432	336	1344
Mlati	110.361	−7.75394	34,703	868	3472
Moyudan	110.239997	−7.772729	11,677	292	1168
Ngaglik	110.378997	−7.743549	39,991	1000	4000
Ngemplak	110.430999	−7.71747	20,906	523	2092
Pakem	110.410003	−7.653709	12,585	315	1260
Prambanan	110.496002	−7.787529	28,141	704	2816
Seyegan	110.299003	−7.72833	17,278	432	1728
Sleman	110.347999	−7.70054	23,814	595	2,380
Tempel	110.317001	−7.670989	19,977	499	1,996
Turi	110.376998	−7.63426	1164	29	116
			380,630	9517	38,068

Source: BPS [125] and spatial analysis of land use data.

This model is also utilised with a synthetic social network, which represents the human relations and spread of risk warning. The social network for the spread of risk warning does not always require physical contact, as in modelling for the spread of disease [126], but can be through non-physical contact, e.g., using the medium of social media [127]. Each agent is assigned with links with other agents in order to mimic social network reality. The number of linked agents is generated differently to accommodate the varying social interactions between people. There are several types of connections among agents: household member connections; friendship connections; and connections with the stakeholder.

3.6. Calibration and Validation

In implementing the model structure discussed above, we need to verify that the model works in line with the concept, as well as fitting the real world. We used the retrodiction approach from the various other validation techniques [51] to measure the validity of the model. This approach focuses on measuring the replicative validity, i.e., the ability of the resulting output from the simulation to match the real data [128]. Two outputs were compared with the real data to establish that the model was plausible: the spatial pattern of reluctant people; and the temporal accumulation of evacuees. If any output was unreasonably different from the real data, we manually adjusted the parameter or the rules of the model to produce reasonable outputs (calibration). Graphical monitor and state chart inspection were used to verify that the implemented model worked corresponding to the model design (visualisation approach) [51]. Calibration and fitting of some parameter values or data was conducted to achieve output similarity (Section 3.6.2). To quantitatively measure the similarity between the modelling output and the real data (Section 3.6.1), we used temporal and spatial validation (Section 3.6.3) [64].

3.6.1. Empirical Data for Comparison

We used several data to measure the validity of the model, including the spatial distribution of reluctant people and the temporal accumulation of evacuees. All these data were provided by the 2010 evacuation records (see Section 3.3). The data on reluctance is provided in Figure 5. Such reluctance always occurs in Merapi based on past eruption records. It also occurred in the 2006 eruption, as identified by Sagala and Okada [35]. Reluctance to evacuate potentially leads to fatalities in disasters; therefore, we considered that validating the model based on this output was important. These data were derived from a map provided by Lavigne et al. [12], which consists of the distribution of villages in which at least one person refused to evacuate in 2010, based on reports from the village chiefs [12]. We selected relevance areas from the original map [12], extracted the centroid of the areas and created the density map (Figure 5) using kernel density analysis in ArcGIS to make a comparison possible with the output of the model [64]. In addition, when people start evacuating (the temporal aspect) is also significant, as late evacuation can also increase risk. Therefore, we also used this issue to measure the validity of the model, where the temporal aspect is expressed as the temporal accumulation of evacuees (Figure 6). This data was from the daily records of evacuees during the eruption of 2010. These records are documented on the government website [129]. These data were copied to Excel and are provided in the supplementary material (Supplementary Material—Appendix 2).

3.6.2. Calibration

We conducted several calibrations to fit the model, as the initial evaluation indicated that there were discrepancies between the simulation results and the real data [15]. The differences were mainly in the comparison of the percentage of the evacuating population, the temporal accumulation of evacuees, and the emergence of reluctant people, which could not be captured in the first model. We assumed that the differences in both the percentage of the evacuating population and the temporal accumulation of evacuees were because of the different hazard scenarios used to make evacuation decisions. The evacuation order in 2010 was based on radius distance, i.e., 20 km from the summit [76].

The population within this radius (Figure 7b) is higher compared to that within the actual hazard zone (Figure 7a), which possibly results in the differences. Based on this assumption, we first calibrated the model by fitting the hazard scenario. We used both hazard zones scenarios (Figure 7) in the simulation and made a comparison of the results. Meanwhile, we addressed the drawback of the first model, which was unable to capture the emergence of reluctance (to evacuate) behaviour, by assigning the evacuation decision (Section 3.4.3), which is the main focus of the paper.

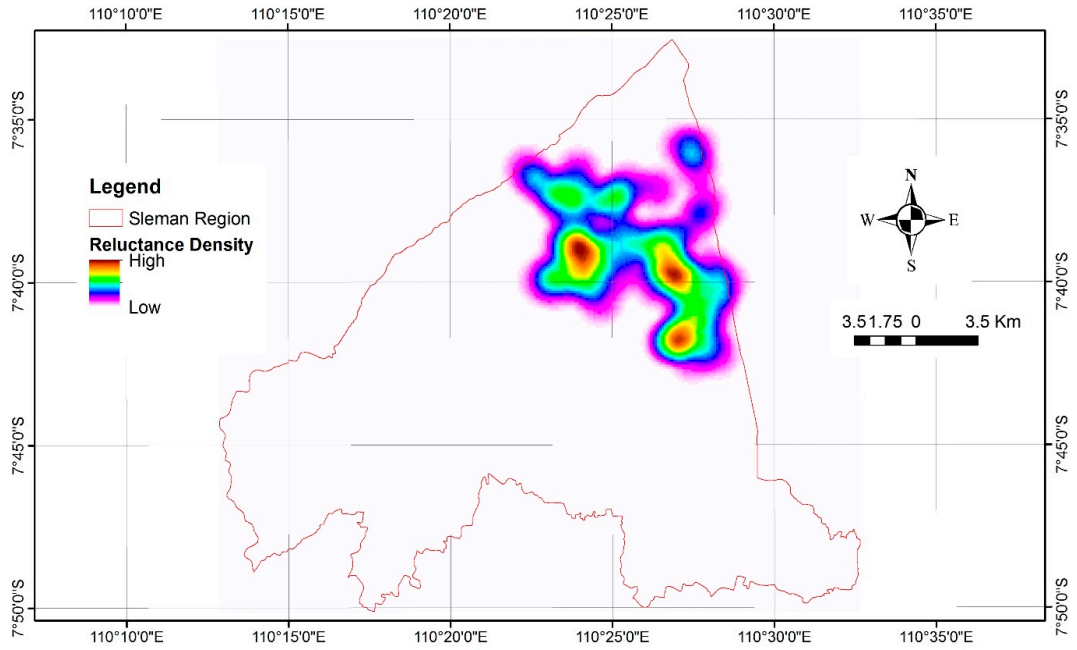

Figure 5. Distribution of reluctant evacuees during the 2010 evacuation (adapted from [12]). The circle shows the 20 km buffer from the summit of the volcano.

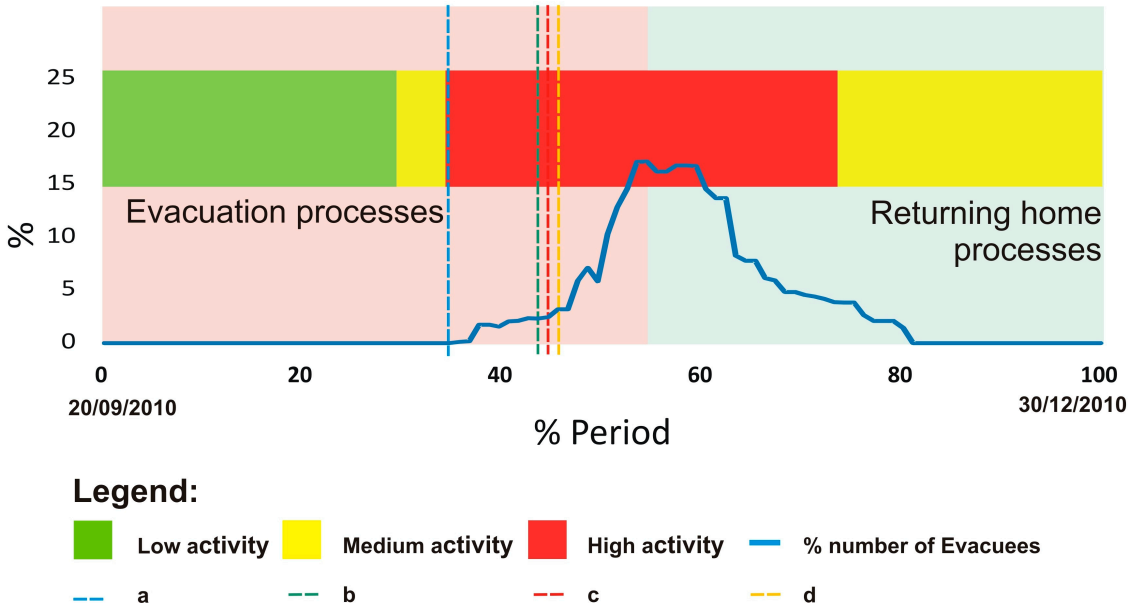

Figure 6. Temporal accumulation of evacuees during the crisis period in 2010. (**a**) Issuance of the first evacuation order on 25 October 2010; (**b**) issuance of a second evacuation order on 3 November 2010; (**c**) major eruption on 4 November 2010; and (**d**) issuance of a third evacuation order on 5 November 2010 (Adapted from [15,76]). Excel data: see Supplementary Material—Appendix 2.

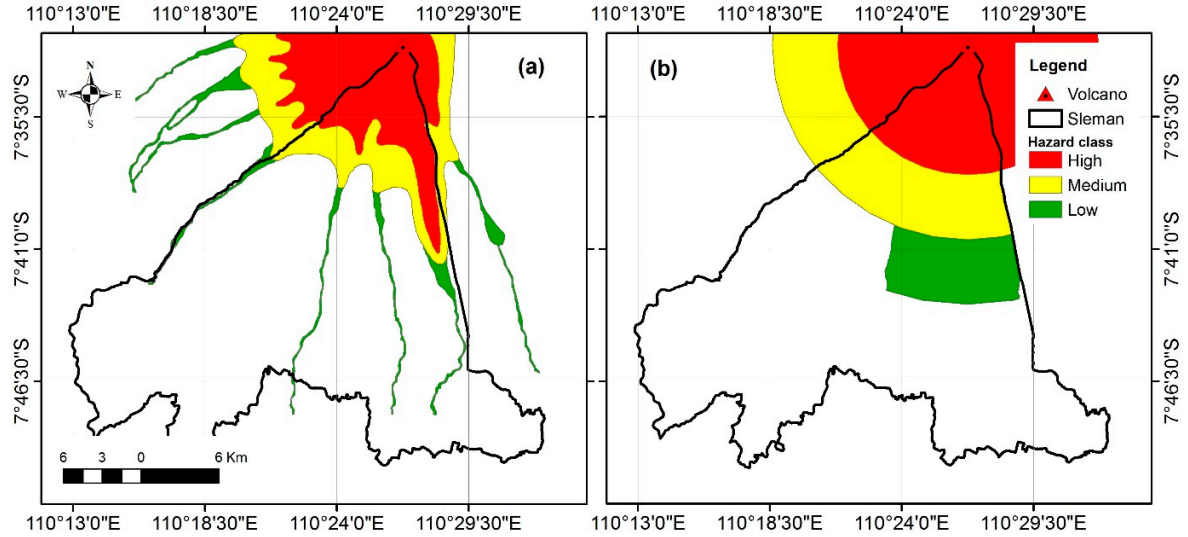

Figure 7. Hazard scenario setting: (**a**) based on actual hazard map [102]; and (**b**) based on hazard map used for evacuation order in 2010 eruption [76].

The simulations were divided into three scenarios with varying parameters. The variation in the settings of these scenarios is provided in Table 7. Scenario 1 uses hazard model a (Figure 7a) to set the hazard zone of the ABM environment. The evacuation decision of this scenario is based on evaluation of the force to evacuate versus the force to stay (Section 3.4.3). However, SE was disregarded in this scenario. Meanwhile, scenario 2 uses hazard model b (Figure 7b) to set the hazardous environment with regard to the SE factor for the decision model. We assumed that this factor was important since the evacuation records from 2010 show that people continued to stay at home after receiving two evacuation alerts from the government, but did evacuate after the major explosion occurred (Figure 6). The scenario uses the same hazard map setting, as well as the same evacuation decision factors, as the second scenario, but different weighting was applied to SI for this scenario.

Table 7. Simulation scenarios.

Scenario	Hazard Model	Weight of Driving Factors to Evacuate (EF)					Weight of Driving Factors to Stay (SF)				
		FD	PI	GA	SI	SE	PP	ND	TC	FS	CB
1	a	1	1	1	1	-	1	1	1	1	1
2	b	1	1	1	1	1	1	1	1	1	1
3	b	1	1	1	1	1.5	1	1	1	1	1

3.6.3. Validation

The validation approach was to make comparisons between the temporal and spatial aspects of the output and the real data. The aim was to assess how well the model predicted the outcome under the same parameters compared to the real event (see Section 3.3 for the data used and Section 3.4.3 for the parameter value setup). We adapted approaches used by Robinson and Rai [64] for the spatial and temporal validation techniques. The spatial validation was conducted to establish the ability of the model to predict the spatial distribution of the reluctant people. Fuzzy similarity (K^*) and a wavelet correlation coefficient (r^w) were used to measure the similarity between the simulation output and the real data [64,130]. We used Map Comparison Kit 3.2 of Visser and Nijs [131] to perform this analysis. Moreover, temporal validation was conducted to establish the ability of the model to represent the time when people start to evacuate. We compared the temporal accumulation of evacuees of both the real and simulation output data. Root mean square error (RMSE) was used to measure the plausibility of this output. We used the rmse library in R [132] to calculate this error for all periods (n = 100) of the

simulated crisis (see Figure 6). The returning home process was excluded in this comparison, since the model only regards the evacuation process (see [15]). When the outputs appeared very different, some parameters/data and rules were calibrated/fitted to obtain the most similar output with the real data. Lastly, we concluded with the most plausible scenario with the indicators being the highest value of K^* and r^w, and the lowest value of RMSE.

4. Results and Discussion

4.1. Results of the Simulation Scenarios

Once the model design (Section 3.4) was applied in the previous model [15], we performed several simulations to verify that the developed model corresponded to the design and that there was no error in the code [133]. After the verification had been conducted and the program ran as intended, we ran the simulation 30 times for each scenario (Section 3.6.2) to provide enough samples for statistical analysis [134,135]. The outputs of the scenarios were analysed and presented both in spatial and temporal distribution. The indicators of the plausibility of the model are presented alongside the results. The results for scenarios 1, 2 and 3 are shown below.

4.1.1. Scenario 1

The first scenario is the basic model of the evacuation decision used in this ABM. Spatial and temporal comparisons between the real data (empirical) and the simulation results of scenario 1 are provided in Figures 8 and 9. The results indicate that the model is able to represent the emergence of reluctant people, as shown in Figure 8. However, the evacuees departed too quickly compared to the empirical data (Figure 9).

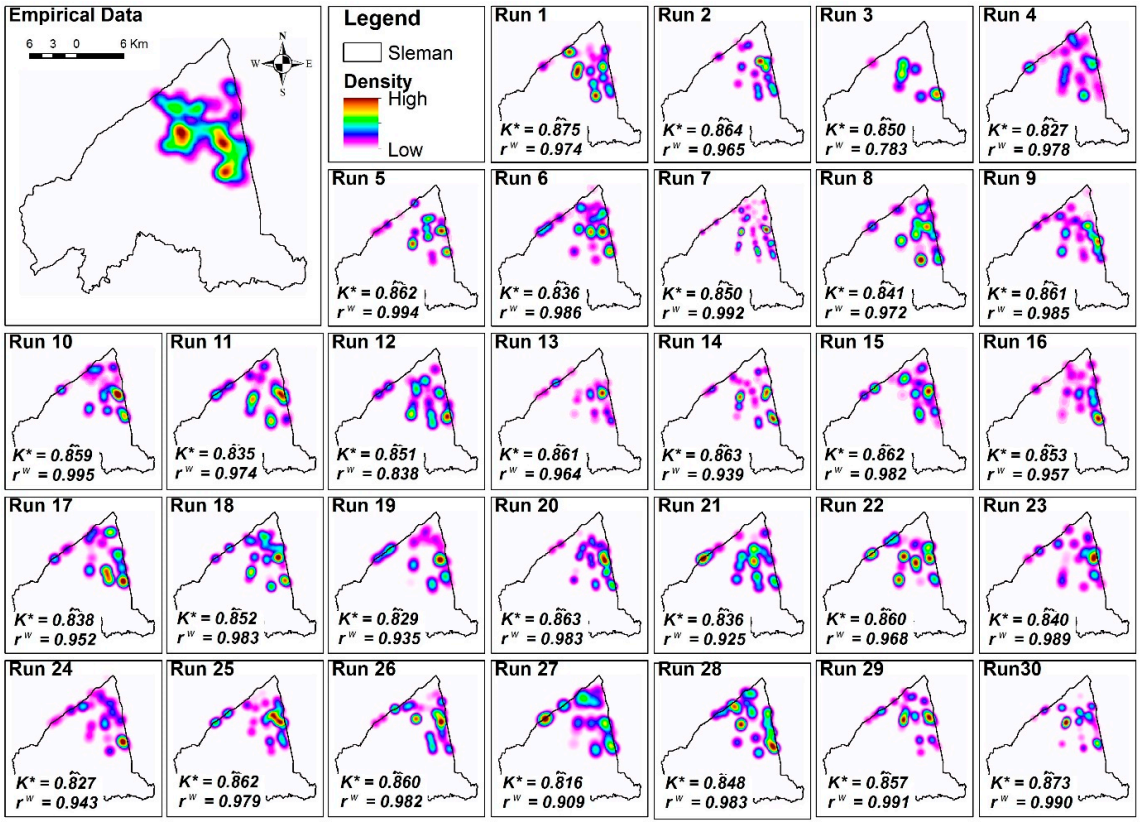

Figure 8. Spatial comparison of simulated and observed reluctance distribution based on scenario 1. The raster data is provided in the supplementary material (Supplementary Material—Appendix 8).

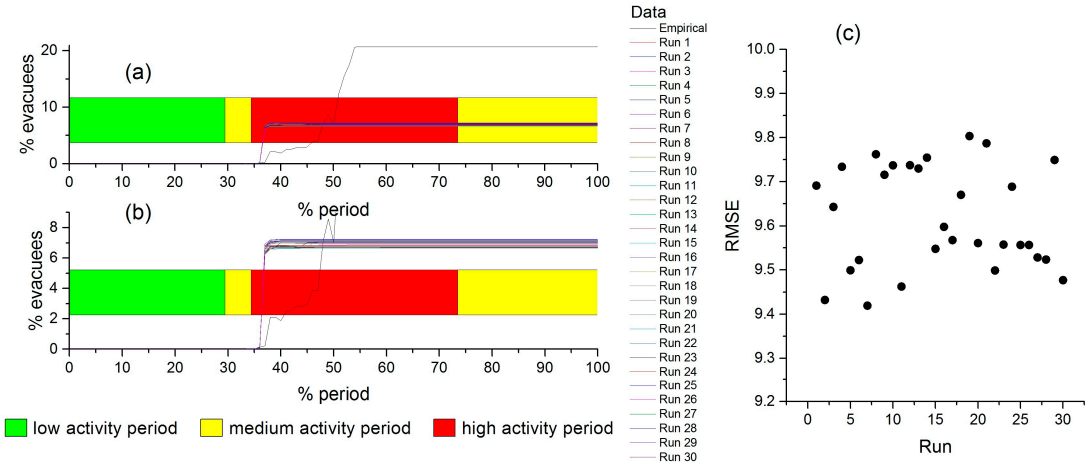

Figure 9. Temporal comparison of simulated and observed evacuee accumulation based on scenario 1: (**a**) overall comparison; (**b**) zoomed to the simulation outputs; and (**c**) RMSEs.

4.1.2. Scenario 2

The second scenario is the improved model, in which both the hazard model and the evacuation decision factors have been adjusted (Section 3.4.3). Spatial and temporal comparison between the real data (empirical) and the simulation results of this scenario are provided in Figures 10 and 11. The results of this scenario also indicate that the model is able to represent the emergence of reluctant people, as shown in Figure 10. The evacuees' departure in this scenario can be classified into two different times: first, roughly half the evacuees departed once the volcanic activity had reached its highest level; second, the remainder departed after the time step reached the major explosion time (Figure 11). This also shows a discrepancy with the empirical data.

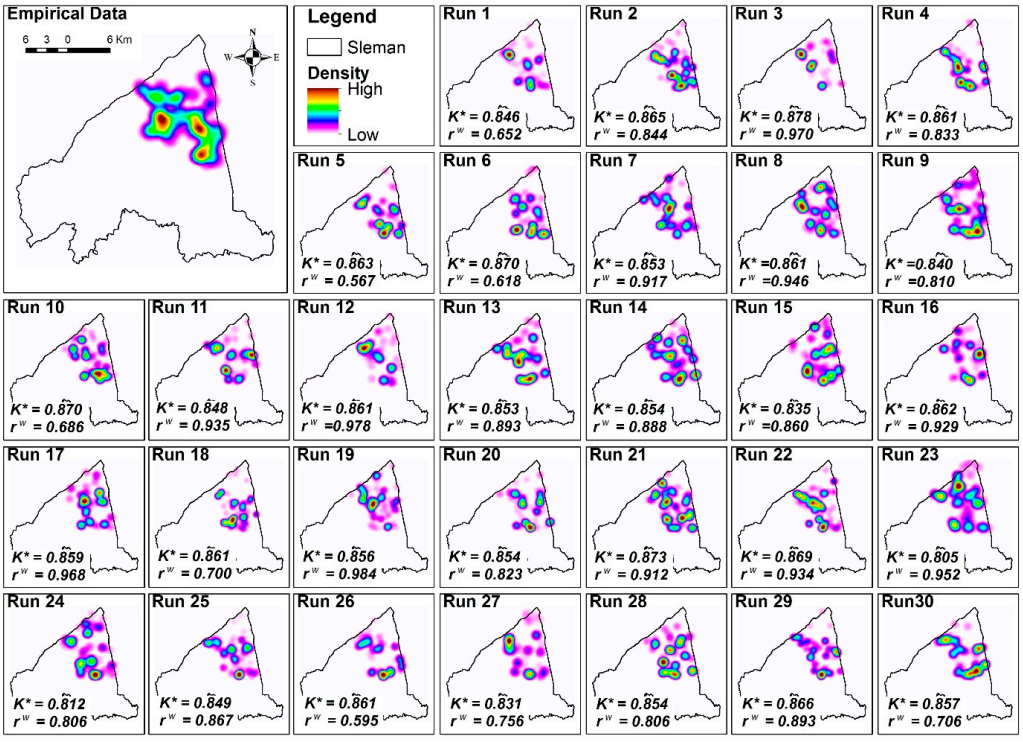

Figure 10. Spatial comparison of simulated and observed reluctance distribution based on scenario 2. The raster data is provided in the supplementary material (Supplementary Material—Appendix 9).

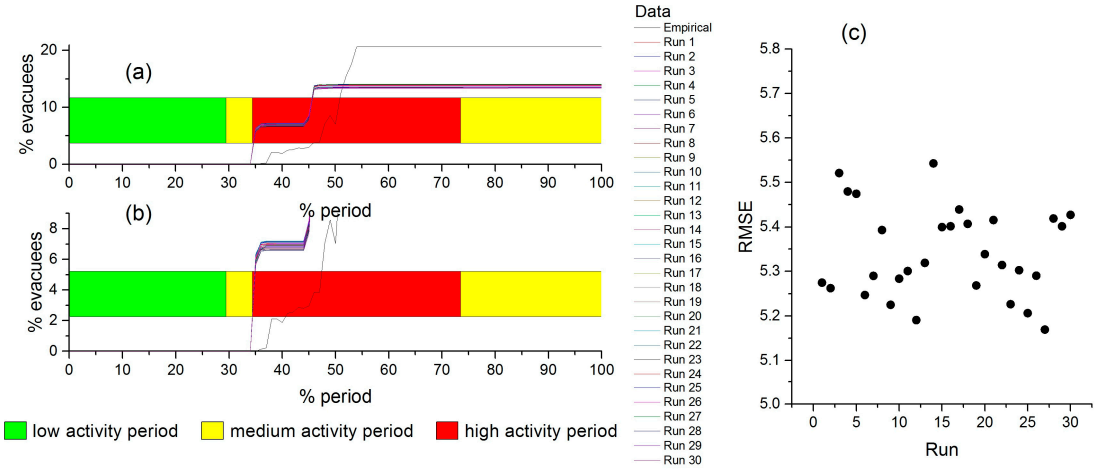

Figure 11. Temporal comparison of simulated and observed evacuee accumulation based on scenario 2: (**a**) overall comparison; (**b**) zoomed to the simulation outputs; and (**c**) RMSEs.

4.1.3. Scenario 3

The third scenario uses a similar hazard and evacuation decision model, but this one has been improved with a weighting strategy for observing the explosion factors (Section 3.4.3). Spatial and temporal comparisons between the real data (empirical) and the simulation results of this scenario are provided in Figures 12 and 13. Similarly, the results of this scenario also indicate that the model is able to represent the emergence of reluctant people, as shown in Figure 12. However, the temporal data shows a different result, that all the evacuees departed after the time step reached the major explosion time (Figure 13). This shows a discrepancy with the empirical data, but appears better than the results of scenarios 1 and 2. Detailed discussion of the comparison between all the scenario results is provided in Section 4.2.

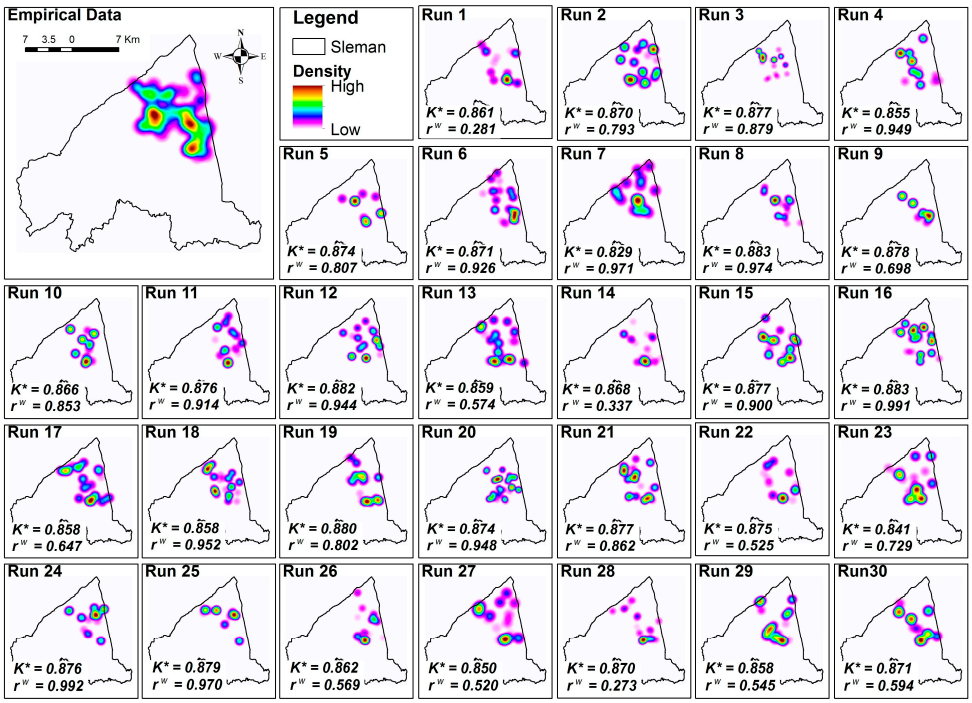

Figure 12. Spatial comparison of simulated and observed reluctance distribution based on scenario 3. The raster data is provided in the supplementary material (Supplementary Material—Appendix 10).

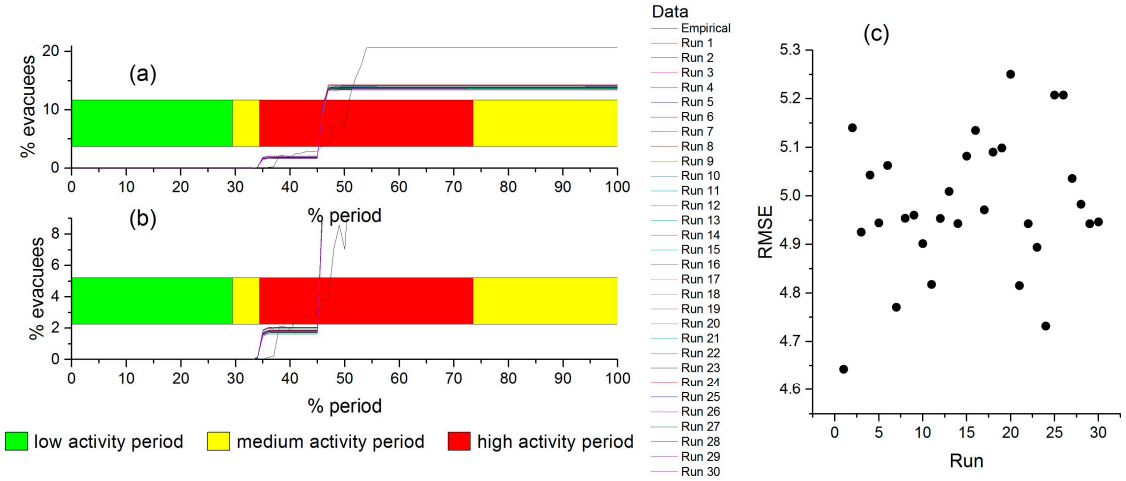

Figure 13. Temporal comparison of simulated and observed evacuee accumulation based on scenario 3: (**a**) overall comparison; (**b**) zoomed to the simulation outputs; and (**c**) RMSEs.

4.2. Discussion and Future Research

An evacuation decision model based on both physical and social factors with three scenarios to fit the model with reality is presented in this paper. The outcome of the research addresses a drawback that was found in the previous model, which was unable to capture the emergence of reluctant people [15]. It also improves on other similar models of evacuation, which give less consideration to this phenomenon (e.g., [13,14,67,127,136]). Additionally, the model has been evaluated through a spatial and temporal validation approach to evaluate its plausibility. The spatial validation is based on evaluation of K^* and r^w [64,130] in the simulated and real spatial distribution of reluctant people. Meanwhile, the temporal validation is based on evaluation of the RMSE [64] of simulated and real temporal accumulation of evacuees (the returning home process is excluded).

There are some studies which help understand these measures (e.g., [64,130,132,137–140]). Fuzzy similarity (K^*) measures the similarity of cells in the same location of one map with their counterparts by taking into account the directly neighbouring cells (local similarity) of the counterpart map based on fuzzy kappa [130,137,140], where the degree of similarity is assigned as 0 (different) or 1 (similar). This means that the higher the value, the more similar the maps. In interpreting the results, a higher value means that the output is more similar to the real data. Meanwhile, the wavelet correlation coefficient (r^w) compares two maps, which are decomposed using a discrete wavelet transform, by RMSE (quantity), r (pattern), and ER (energy) [130]. This paper focuses on pattern comparison, therefore, an r coefficient is used for the measurement. Similar to K^*, the degree of similarity of this is also assigned as 0 or 1, in which a higher correlation means the greater the similarity of the pattern. Both K^* and r^w measure the degree of similarity based on the equivalency of the structures of the maps, where the individual values may not exactly be the same [140]. r^w is used together with K^* to measure the robustness of the results; if the r^w value is consistent with K^* this means that the similarity of the simulation output with the real data is robust [140]. On the other hand, the RMSE that is used to measure temporal validity measures the deviation of the output of the simulation from the real data [140]. A smaller value means better mimicry of the real data.

Based on the evaluations and measurements, all the scenarios presented here are able to simulate the emergence of reluctant people, which is the main objective of this paper. The first scenario is the most robust of all, with the value of K^* consistent with r^w. However, the third scenario is the most plausible, based on the evaluation of both the spatial and temporal validation results. However, this is not the best scenario as evaluated from one aspect, i.e., spatial validation. Based on the visual inspection of Figure 14 to provide a qualitative comparison [141], this indicates that the second model is the most appropriate, but the statistical analysis shows differences. The statistical analysis of K^* and

r^w shown in Figure 15a indicate that the first scenario gives the best outcome. This is indicated not only from the values of both K^* and r^w, but also from the ranges of the values; their values in this scenario are relatively higher than those in the other scenarios. In addition, these have the smallest of all the ranges (minimum variation). Moreover, both values in this scenario are the most consistent compared to the others; the outcomes from the other scenarios show variance between K^* and r^w. However, the temporal validation (Figure 15b) indicates that the first scenario results in the highest error (RMSE), while the third scenario give the best results based on both the values and the range from the simulation results. Based on this, and its spatial validation results which are still reasonable compared to the others, the third scenario can better represent a real evacuation.

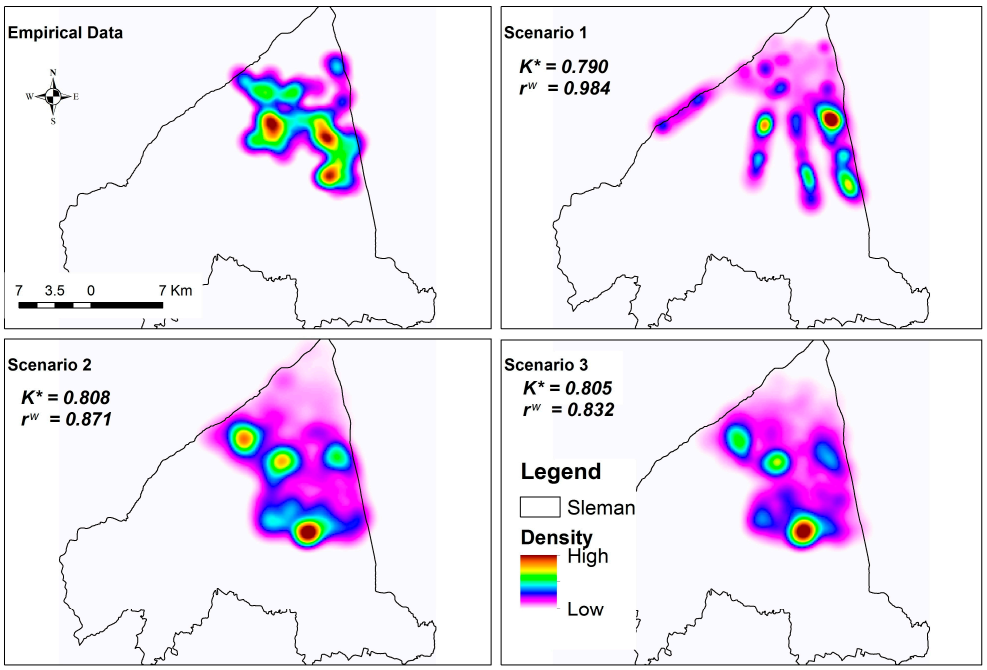

Figure 14. Overall comparison of spatial distribution of reluctant people. The scenario output was averaged.

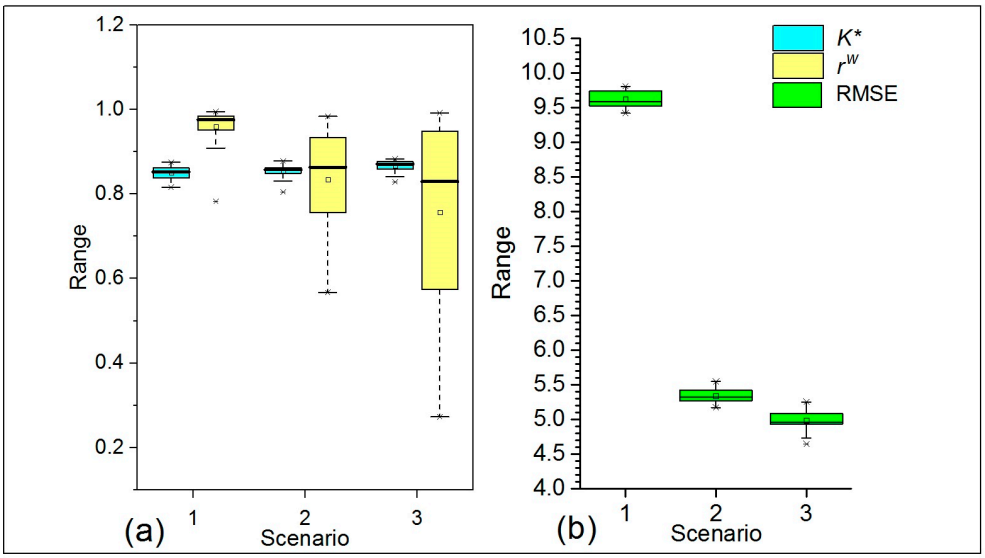

Figure 15. Comparison of both spatial and temporal measures of validity for all scenarios. (**a**) Spatial validity evaluation based on K^* and r^w; and (**b**) temporal validity evaluation based on RMSE.

We found from this model evaluation that the occurrence of disaster can be a major factor to evacuate. This is proved in this model, as the results more closely fit reality after this aspect (explosion occurrence) was weighted (Scenario 3) in the case study (see Figures 6 and 13). People are likely to disobey the evacuation command, but are motivated to evacuate after the real explosion has occurred (Figure 6). Such difficulties in ordering people to evacuate is a common phenomenon [142]. It occurs not only in the case of volcanic eruption, but also in the other hazards, such as Hurricane Katrina [143]. Therefore, a strong evacuation command is needed to ensure the evacuation processes [144]; for example, military force, as in the evacuation from Tungurahua, Ecuador in 1999 [142]. Nevertheless, although this evaluation indicates that explosion (occurrence of disaster) is the major motivation to evacuate, we still lack information on why there is a delay between the major explosion and the evacuation, as indicated in Figure 6. This missing information makes it impossible to model this delay in the current design.

Furthermore, a thorough evacuation decision should also include a decision on destination choice. This has also been assigned in this model, but has yet to be calibrated or validated. It is important to compare the distribution of evacuees with the real data as this expresses the validity of the destination choice rule of the agent. In 2010, the population within the danger zone in Merapi evacuated to temporary shelters (evacuation centres) distributed outside the danger zone (Figure 16). These shelters were commonly public facilities, such as stadiums, schools, mosques/churches, etc. Analysing the distribution of evacuees in Figure 16, it can be assumed that the majority from Merapi selected the nearest shelter as their destination (travel distance). This is proven by the fact that the percentage occupancy of the shelters in the surroundings of the restricted zone were relatively high compared to more distant ones. Some people chose shelters close to public services. Interestingly, there are many small numbers that chose quite remote spots as their destination. Commonly, evacuees chose this kind of shelter because they had relatives in the destination area [145,146] or they were looking for a safer place [147], which is relevant to the finding by Cheng et al. [148]. In Merapi, based on the shelter zoning analysis of Figure 16, 80.3% of evacuees preferred to select the shortest distance, 12.4% preferred to select destinations close to public services zones, and the rest (7.2%) either used relatives or risk indicators as preferences. This issue, together with involving the delay factors as mentioned earlier, would be good future directions to improve this model.

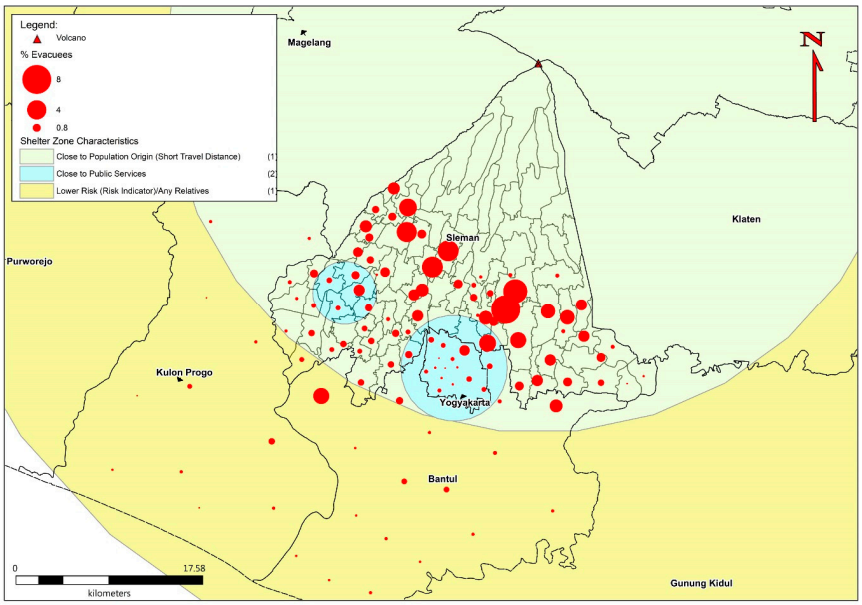

Figure 16. Distribution of evacuees from Sleman in the 2010 Merapi crisis. Source: Geospatial BNPB [104–107], DYMDIS GEGAMA [108]. The shapefile is provided in Supplementary Material—Appendix 11.

5. Conclusions

The paper presented an individual evacuation decision model in ABM with Mt. Merapi, Indonesia as a case study. The model was based on various interrelating factors developed from the literature review and survey. These factors were categorized into driving forces to evacuate or driving forces to stay. The threshold-based approach was used to evaluate the differences in both values and to define whether agents would evacuate or stay. This decision model can be used to simulate two important aspects of evacuation, namely, the dynamic of evacuation departure, and the emergence of reluctant people. Both of these aspects are important in defining the effectiveness of evacuation because a high emergence of reluctant people or evacuation which is too late will increase the risk. Calibration was conducted by setting up the parameters based on three scenarios. We validated the model by a retrodiction approach, which consisted of spatial and temporal validation. K^* and r^w were used to measure the validity of the spatial distribution of the simulated reluctant people against the real data. Meanwhile, RMSE was used to measure the validity of the temporal accumulation of evacuees. Analysis of the simulation outputs shows that scenario 3, which weighted the occurrence of an explosion as the most important motivation for evacuation (four times more important than the other aspects), was the most plausible model in mimicking the real volcanic disaster events in Mt. Merapi. This plausibility was indicated by both the spatial and temporal similarity of the output with the real data being relatively high (high K^*, r^w, and low RMSE) compared to the other scenarios.

Supplementary Materials: (1) Appendix 1. Statistical Analysis of Survey Data (https://osf.io/a8zew/); (2) Appendix 2. Evacuation Dataset (https://osf.io/4kujy/); (3) Appendix 3. Reluctance Raster Map (https://osf.io/gy8ew/); (4) Appendix 4. Functions Overview of Evacuation Decision for Scenario 1 (https://osf.io/pqmv3/); (5) Appendix 5. Functions Overview of Evacuation Decision for Scenario 2 (https://osf.io/tkanc/); (6) Appendix 6. Functions Overview of Evacuation Decision for Scenario 3 (https://osf.io/rcqb3/); (7) Appendix 7. Main state chart diagram of the evacuation decision (https://osf.io/wftx7/); (8) Raster data for Figure 9 (https://osf.io/chgdy/); (9) Raster data for Figure 11 (https://osf.io/cygmp/); (10) Raster data for Figure 13 (https://osf.io/3jvhb/); (11) Shapefile for Figure 16 (https://osf.io/4upe9/).

Author Contributions: J. collected and analysed the dataset; S.J.C., D.J.Q., N.S.M. and V.R.M. advised on the data collection; J. conceived, designed, and performed the experiments; and analysed the output; A.J.H., N.S.M., S.J.C. and D.J.Q. helped in improving the model design; J. wrote the manuscript; and J., A.J.H., N.S.M., S.J.C., D.J.Q. and V.R.M. improved the manuscript. All the authors read and approved the final manuscript.

Acknowledgments: This article is part of the PhD project of the main author in the School of Geography, University of Leeds. We gratefully acknowledge the Indonesian Ministry of Research and Higher Education for the funding through the Directorate General of Higher Education (DGHE) scholarship (BPPLN-DIKTI). Thanks to Seftiawan Samsu Rijal, Syarif Hidayat, Rudiyanto, Rahit Iskandar, and Ambar Asmoro's Team who supported data collections. We also would like to acknowledge the anonymous reviewers for the valuable feedbacks.

Conflicts of Interest: The authors declare no conflict of interest.

References

1. Alcántara-Ayala, I. Geomorphology, natural hazards, vulnerability and prevention of natural disasters in developing countries. *Geomorphology* **2002**, *47*, 107–124. [CrossRef]
2. Beck, U. *World at Risk*; Polity: Cambridge, UK, 2009.
3. CRED. *2015 Disasters in Numbers 2016*; CRED: Brussels, Belgium, 2016.
4. Guha-Sapir, D.; Hoyois, P.; Below, R. *Annual Disaster Statistical Review 2015*; CRED: Brussels, Belgium, 2016.
5. Siagian, T.H.; Purhadi, P.; Suhartono, S.; Ritonga, H. Social vulnerability to natural hazards in Indonesia: Driving factors and policy implications. *Nat. Hazards* **2013**, *70*, 1603–1617. [CrossRef]
6. Makinoshima, F.; Abe, Y.; Imamura, F.; Machida, G.; Takeshita, Y. Possible Factors Promoting Car Evacuation in the 2011 Tohoku Tsunami Revealed by Analysing a Large-Scale Questionnaire Survey in Kesennuma City. *Geosciences* **2017**, *7*, 112. [CrossRef]
7. Quarantelli, E.L. *The Warning Process and Evacuation Behavior: The Research Evidence*; Disaster Research Center: Newark, Delaware, 1990.
8. Saadatseresht, M.; Mansourian, A.; Taleai, M. Evacuation planning using multiobjective evolutionary optimization approach. *Eur. J. Oper. Res.* **2009**, *198*, 305–314. [CrossRef]

9. Cutter, S.L.; Barnes, L.; Berry, M.; Burton, C.; Evans, E.; Tate, E.; Webb, J. A place-based model for understanding community resilience to natural disasters. *Glob. Environ. Chang.* **2008**, *18*, 598–606. [CrossRef]
10. Voight, B.; Constantine, E.K.; Siswowidjoyo, S.; Torley, R. Historical eruptions of Merapi Volcano, Central Java, Indonesia, 1768–1998. *J. Volcanol. Geotherm. Res.* **2000**, *100*, 69–138. [CrossRef]
11. Mei, E.T.W.; Lavigne, F. Influence of the institutional and socio-economic context for responding to disasters: Case study of the 1994 and 2006 eruptions of the Merapi Volcano, Indonesia. *Geol. Soc. Lond. Spec. Publ.* **2012**, *361*, 171–186. [CrossRef]
12. Lavigne, F.; Morin, J.; Mei, E.T.W.; Calder, E.S.; Usamah, M.; Nugroho, U. Mapping hazard zones, rapid warning communication and understanding communities: Primary ways to mitigate pyroclastic flow hazard. In *Advances in Volcanology*; Springer: Berlin/Heidelberg, Germany, 2017; pp. 1–13.
13. Zhang, B.; Chan, W.K.; Ukkusuri, S.V. Agent-based modeling for household level hurricane evacuation. In Proceedings of the 2009 Winter Simulation Conference (WSC), Austin, TX, USA, 13–16 December 2009; pp. 2778–2784.
14. Mas, E.; Suppasri, A.; Imamura, F.; Koshimura, S. Agent-based simulation of the 2011 great east japan earthquake/tsunami evacuation: An integrated model of tsunami inundation and evacuation. *J. Nat. Disaster Sci.* **2012**, *34*, 41–57. [CrossRef]
15. Carver, S.; Quincey, D. A Conceptual Design of Spatio-Temporal Agent-Based Model for Volcanic Evacuation. *Systems* **2017**, *5*, 53. [CrossRef]
16. Chen, X.; Zhan, F.B. Agent-based modelling and simulation of urban evacuation: Relative effectiveness of simultaneous and staged evacuation strategies. *J. Oper. Res. Soc.* **2008**, *59*, 25–33. [CrossRef]
17. Chandan, S.; Saha, S.; Barrett, C.; Eubank, S.; Marathe, A.; Marathe, M.; Swarup, S.; Vullikanti, A.K.S. Modeling the interaction between emergency communications and behavior in the aftermath of a disaster. In Proceedings of the International Conference on Social Computing, Behavioral-Cultural Modeling, and Prediction, Washington, DC, USA, 2–5 April 2013; Springer: Berlin, Germany, 2013; pp. 476–485.
18. Donovan, K. Cultural Responses to Volcanic Hazards on Mt Merapi, Indonesia. Ph.D. Thesis, University of Plymouth, Plymouth, UK, 2010.
19. Sagala, S.A.H. System Analysis of Social Resilience against Volcanic Risks Case Studies of Merapi, Indonesia and Mt. Sakurajima, Japan. Ph.D. Thesis, Kyoto University, Kyoto, Japan, 2009.
20. Wilson, T.; Cole, J.; Johnston, D.; Cronin, S.; Stewart, C.; Dantas, A. Short- and long-term evacuation of people and livestock during a volcanic crisis: Lessons from the 1991 eruption of Volcán Hudson, Chile. *J. Appl. Volcanol.* **2012**, *1*, 2. [CrossRef]
21. Grimm, V.; Berger, U.; Bastiansen, F.; Eliassen, S.; Ginot, V.; Giske, J.; Goss-Custard, J.; Grand, T.; Heinz, S.K.; Huse, G.; et al. A standard protocol for describing individual-based and agent-based models. *Ecol. Model.* **2006**, *198*, 115–126. [CrossRef]
22. Polhill, J.G. ODD Updated. *J. Artif. Soc. Soc. Simul.* **2010**, *13*, 9. [CrossRef]
23. Dash, N.; Gladwin, H. Evacuation Decision Making and Behavioral Responses: Individual and Household. *Nat. Hazards Rev.* **2007**, *8*, 69–77. [CrossRef]
24. Ahsan, M.N.; Takeuchi, K.; Vink, K.; Ohara, M. A Systematic Review of the Factors Affecting the Cyclone Evacuation Decision Process in Bangladesh. *J. Disaster Res.* **2016**, *11*, 741. [CrossRef]
25. Lim, M.B.B.; Lim, H.R.; Piantanakulchai, M.; Uy, F.A. A household-level flood evacuation decision model in Quezon City, Philippines. *Nat. Hazards* **2015**, *80*, 1539–1561. [CrossRef]
26. Linardi, S. Peer coordination and communication following disaster warnings: An experimental framework. *Saf. Sci.* **2016**. [CrossRef]
27. Siebeneck, L.K.; Cova, T.J. Spatial and temporal variation in evacuee risk perception throughout the evacuation and return-entry process. *Risk Anal.* **2012**, *32*, 1468–1480. [CrossRef] [PubMed]
28. Golledge, R.G. *Spatial Behavior: A Geographic Perspective*; Guilford Press: New York, NY, USA, 1997.
29. Ronald, W. Population Evacuation in Volcanic Eruptions, Floods, and Nuclear Power Plant Accidents: Some Elementary Comparisons. *J. Community Pschol.* **1983**, *11*, 36–47.
30. Botzen, W.J.; Aerts, J.C.; van den Bergh, J.C. Dependence of flood risk perceptions on socioeconomic and objective risk factors. *Water Resour. Res.* **2009**, *45*. [CrossRef]
31. Bird, D.K.; Gísladóttir, G.; Dominey-Howes, D. Different communities, different perspectives: Issues affecting residents' response to a volcanic eruption in southern Iceland. *Bull. Volcanol.* **2011**, *73*, 1209–1227. [CrossRef]

32. Rianto, T. Spatial Analysis of Volcanic Risk Perception Case Study in Local Community at Merapi Volcano Dangerous Zones. Master's Thesis, ITC, University of Twente, Enschede, The Netherlands, 2009.
33. Khalid, M.N.A.; Yusof, U.K. A Crowd Modelling Considering Group Cohesion in the Emergency Route Planning Problems. *Aust. J. Basic Appl. Sci.* **2014**, *8*, 33–39.
34. Liu, S.; Murray-Tuite, P.; Schweitzer, L. Incorporating Household Gathering and Mode Decisions in Large-Scale No-Notice Evacuation Modeling. *Comput.-Aided Civ. Infrastruct. Eng.* **2014**, *29*, 107–122. [CrossRef]
35. Sagala, S.; Okada, N. F-2 Statistical analysis of correlation between hazard-related factors and households' evacuation decisions in Mt. Merapi. *Proc. Annu. Conf. Inst. Soc. Saf. Sci.* **2009**, *AA12381938*, 61–64.
36. Donovan, K. Doing social volcanology: Exploring volcanic culture in Indonesia. *Area* **2010**, *42*, 117–126. [CrossRef]
37. Lavigne, F.; De Coster, B.; Juvin, N.; Flohic, F.; Gaillard, J.-C.; Texier, P.; Morin, J.; Sartohadi, J. People's behaviour in the face of volcanic hazards: Perspectives from Javanese communities, Indonesia. *J. Volcanol. Geotherm. Res.* **2008**, *172*, 273–287. [CrossRef]
38. Tayag, J.; Insauriga, S.; Ringor, A.; Belo, M. People's response to eruption warning: The Pinatubo experience, 1991–1992. In *Fire and mud. Eruptions and Lahars of Mount Pinatubo, Philippines*; University of Washington Press: Seattle, WC, USA, 1996.
39. Canessa, E.; Riolo, R.L. The effect of organizational communication media on organizational culture and performance: An agent-based simulation model. *Comput. Math. Organ. Theory* **2003**, *9*, 147–176. [CrossRef]
40. Marsella, S.C.; Pynadath, D.V.; Read, S.J. PsychSim: Agent-based modeling of social interactions and influence. In Proceedings of the International Conference on Cognitive Modeling, Pittsburgh, PA, USA, 30 July–1 August 2004; Volume 36, pp. 243–248.
41. Qiu, F.; Hu, X. Modeling group structures in pedestrian crowd simulation. *Simul. Model. Pract. Theory* **2010**, *18*, 190–205. [CrossRef]
42. Reneke, P.A. *Evacuation Decision Model*; US Department of Commerce, National Institute of Standards and Technology: Washington, DC, USA, 2013.
43. Lovreglio, R.; Ronchi, E.; Nilsson, D. An Evacuation Decision Model based on perceived risk, social influence and behavioural uncertainty. *Simul. Model. Pract. Theory* **2016**. [CrossRef]
44. Rosenbaum, M.S.; Culshaw, M.G. Communicating the Risks Arising from Geohazards. *J. R. Stat. Soc. Ser. A Stat. Soc.* **2003**, *166*, 261–270. [CrossRef]
45. Macal, C.M.; North, M.J. Tutorial on agent-based modeling and simulation. In Proceedings of the 37th Conference on Winter Simulation, Orlando, FL, USA, 4–7 December 2005; pp. 2–15.
46. Gilbert, G.N. *Agent-Based Models*; SAGE: London, UK, 2008; ISBN 978-1-4129-4964-4.
47. Macal, C.M. Model verification and validation. In Proceedings of the Workshop on Threat Anticipation: Social Science Methods and Models, Chicago, IL, USA, 7–8 April 2005.
48. Brown, D.G.; Xie, Y. Spatial agent-based modelling. *Int. J. Geogr. Inf. Sci.* **2006**, *20*, 941–943. [CrossRef]
49. Pons, M.; Johnson, P.A.; Rosas, M.; Jover, E. A georeferenced agent-based model to analyze the climate change impacts on ski tourism at a regional scale. *Int. J. Geogr. Inf. Sci.* **2014**, *28*, 2474–2494. [CrossRef]
50. Brown, D.G.; Riolo, R.; Robinson, D.T.; North, M.; Rand, W. Spatial process and data models: Toward integration of agent-based models and GIS. *J. Geogr. Syst.* **2005**, *7*, 25–47. [CrossRef]
51. Hawe, G.I.; Coates, G.; Wilson, D.T.; Crouch, R.S. Agent-based simulation for large-scale emergency response: A survey of usage and implementation. *ACM Comput. Surv. CSUR* **2012**, *45*, 8. [CrossRef]
52. Zheng, X.; Zhong, T.; Liu, M. Modeling crowd evacuation of a building based on seven methodological approaches. *Build. Environ.* **2009**, *44*, 437–445. [CrossRef]
53. Cole, J.W.; Sabel, C.E.; Blumenthal, E.; Finnis, K.; Dantas, A.; Barnard, S.; Johnston, D.M. GIS-Based Emergency and Evacuation Planning for Volcanic Hazards in New Zealand. 2005. Available online: http://www.nzsee.org.nz (accessed on 20 March 2018).
54. Marrero, J.M.; García, A.; Llinares, A.; Rodríguez-Losada, J.A.; Ortiz, R. The Variable Scale Evacuation Model (VSEM): A new tool for simulating massive evacuation processes during volcanic crises. *Nat. Hazards Earth Syst. Sci.* **2010**, *10*, 747–760. [CrossRef]
55. Wang, D.Q.; Gong, Q.G.; Shen, X.F. An Improved Personnel Evacuation Cellular Automata Model Based on the Ant Colony Optimization Algorithm. *Appl. Mech. Mater.* **2014**, *513–517*, 3287–3291. [CrossRef]

56. Ye, Z.; Yin, Y.; Zong, X.; Wang, M. An Optimization model for evacuation based on cellular automata and ant colony algorithm. In Proceedings of the 2014 Seventh International Symposium on Computational Intelligence and Design (ISCID), Hangzhou, China, 13–14 December 2014; Volume 1, pp. 7–10.
57. Yuan, W.; Tan, K.H. An evacuation model using cellular automata. *Phys. Stat. Mech. Appl.* **2007**, *384*, 549–566. [CrossRef]
58. Bonabeau, E. Agent-based modeling: Methods and techniques for simulating human systems. *Proc. Natl. Acad. Sci. USA* **2002**, *99*, 7280–7287. [CrossRef] [PubMed]
59. Reynolds, C. Individual-Based Models. 1999. Available online: http://www.red3d.com/cwr/ibm.html (accessed on 14 April 2017).
60. An, L. Modeling human decisions in coupled human and natural systems: Review of agent-based models. *Ecol. Model.* **2012**, *229*, 25–36. [CrossRef]
61. Chapuis, K.; Taillandier, P.; Renaud, M.; Drogoul, A. Gen*: A generic toolkit to generate spatially explicit synthetic populations. *Int. J. Geogr. Inf. Sci.* **2018**, *32*, 1194–1210. [CrossRef]
62. Gilbert, N. Computer Simulation of Social Processes. 1993. Available online: http://sru.soc.surrey.ac.uk/SRU6.html (accessed on 14 April 2017).
63. Klügl, F. A validation methodology for agent-based simulations. In Proceedings of the 2008 ACM Symposium on Applied Computing (SAC '08), Fortaleza, Ceara, Brazil, 16–20 March 2008; ACM: New York, NY, USA, 2008; pp. 39–43.
64. Robinson, S.A.; Rai, V. Determinants of spatio-temporal patterns of energy technology adoption: An agent-based modeling approach. *Appl. Energy* **2015**, *151*, 273–284. [CrossRef]
65. Heppenstall, A.; Malleson, N.; Crooks, A. "Space, the Final Frontier": How Good are Agent-Based Models at Simulating Individuals and Space in Cities? *Systems* **2016**, *4*, 9. [CrossRef]
66. Lee, J.-S.; Filatova, T.; Ligmann-Zielinska, A.; Hassani-Mahmooei, B.; Stonedahl, F.; Lorscheid, I.; Voinov, A.; Polhill, J.G.; Sun, Z.; Parker, D.C. The Complexities of Agent-Based Modeling Output Analysis. *J. Artif. Soc. Soc. Simul.* **2015**, *18*, 4. [CrossRef]
67. Wang, H.; Mostafizi, A.; Cramer, L.A.; Cox, D.; Park, H. An agent-based model of a multimodal near-field tsunami evacuation: Decision-making and life safety. *Transp. Res. Part C Emerg. Technol.* **2016**, *64*, 86–100. [CrossRef]
68. Christensen, K.; Sasaki, Y. Agent-Based Emergency Evacuation Simulation with Individuals with Disabilities in the Population. Available online: http://jasss.soc.surrey.ac.uk/11/3/9.html (accessed on 17 March 2015).
69. Shi, J.; Ren, A.; Chen, C. Agent-based evacuation model of large public buildings under fire conditions. *Autom. Constr.* **2009**, *18*, 338–347. [CrossRef]
70. Tan, L.; Hu, M.; Lin, H. Agent-based simulation of building evacuation: Combining human behavior with predictable spatial accessibility in a fire emergency. *Inf. Sci.* **2015**, *295*, 53–66. [CrossRef]
71. Zhao, H.; Winter, S.; Tomko, M. Integrating Decentralized Indoor Evacuation with Information Depositories in the Field. *ISPRS Int. J. Geo-Inf.* **2017**, *6*, 213. [CrossRef]
72. Cajka, J.C.; Cooley, P.C.; Wheaton, W.D. *Attribute Assignment to a Synthetic Population in Support of Agent-Based Disease Modeling*; Methods Report; RTI Press: Research Triangle Park, NC, USA, 2010; Volume 19, pp. 1–14. [PubMed]
73. Malleson, N.; Birkin, M. Analysis of crime patterns through the integration of an agent-based model and a population microsimulation. *Comput. Environ. Urban Syst.* **2012**, *36*, 551–561. [CrossRef]
74. Namazi-Rad, M.-R.; Huynh, N.; Barthelemy, J.; Perez, P. Synthetic population initialization and evolution-agent-based modelling of population aging and household transitions. In Proceedings of the International Conference on Principles and Practice of Multi-Agent Systems, Gold Coast, QLD, Australia, 1–5 December 2014; pp. 182–189.
75. Sadono, R.; Hartono, H.; Machfoedz, M.M.; Setiaji, S. Monitoring Land Cover Changes in the Disaster-Prone Area: A Case Study of Cangkringan Sub-District, the Flanks of Mount Merapi, Indonesia. *Forum Geogr.* **2017**, *31*. [CrossRef]
76. Mei, E.T.W.; Lavigne, F.; Picquout, A.; de Bélizal, E.; Brunstein, D.; Grancher, D.; Sartohadi, J.; Cholik, N.; Vidal, C. Lessons learned from the 2010 evacuations at Merapi volcano. *J. Volcanol. Geotherm. Res.* **2013**, *261*, 348–365. [CrossRef]

77. Mei, E.T.W.; Lavigne, F.; Picquout, A.; Grancher, D. Crisis management during the 2010 Eruption of Merapi Volcano. In Proceedings of the Regional Geographic Conference—International Geographical Union, Santiago, Chile, 14–18 November 2011; pp. 15–19.
78. Siebert, L.; Simkin, T.; Kimberly, P. *Volcanoes of the World*; University of California Press: Berkeley, CA, USA, 2011.
79. Newhall, C.G.; Self, S. The volcanic explosivity index (VEI) an estimate of explosive magnitude for historical volcanism. *J. Geophys. Res.* **1982**, *87*, 1231. [CrossRef]
80. Gertisser, R.; Charbonnier, S.J.; Keller, J.; Quidelleur, X. The geological evolution of Merapi volcano, Central Java, Indonesia. *Bull. Volcanol.* **2012**, *74*, 1213–1233. [CrossRef]
81. Thouret, J.-C.; Lavigne, F.; Kelfoun, K.; Bronto, S. Toward a revised hazard assessment at Merapi volcano, Central Java. *J. Volcanol. Geotherm. Res.* **2000**, *100*, 479–502. [CrossRef]
82. Wilson, T.; Kaye, G.; Stewart, C.; Cole, J. *Impacts of the 2006 Eruption of Merapi Volcano, Indonesia, on Agriculture and Infrastructure*; GNS Science Report 2007/07; Institute of Geological and Nuclear Sciences Limited: Lower Hutt, New Zealand, 2007; p. 69.
83. Jousset, P.; Pallister, J.; Boichu, M.; Buongiorno, M.F.; Budisantoso, A.; Costa, F.; Andreastuti, S.; Prata, F.; Schneider, D.; Clarisse, L.; et al. The 2010 explosive eruption of Java's Merapi volcano—A '100-year' event. *J. Volcanol. Geotherm. Res.* **2012**, *241–242*, 121–135. [CrossRef]
84. Marfai, M.A.; Cahyadi, A.; Hadmoko, D.S.; Sekaranom, A.B. Sejarah Letusan Gunung Merapi Berdasarkan Fasies Gunungapi di Daerah Aliran Sungai Bedog, Daerah Istimewa Yogyakarta. *RISET Geologi dan Pertambangan* **2012**, *22*, 73–80. [CrossRef]
85. Branney, M.; Kokelaar, B.P. Sedimentation of ignimbrites from pyroclastic density currents. *Mem. Geol. Soc. Lond.* **2002**, *27*, 150.
86. Bardintzeff, J.M. Merapi volcano (Java, Indonesia) and Merapi-type nuée ardente. *Bull. Volcanol.* **1984**, *47*, 433–446. [CrossRef]
87. Charbonnier, S.J.; Gertisser, R. Field observations and surface characteristics of pristine block-and-ash flow deposits from the 2006 eruption of Merapi Volcano, Java, Indonesia. *J. Volcanol. Geotherm. Res.* **2008**, *177*, 971–982. [CrossRef]
88. Solikhin, A.; Pinel, V.; Vandemeulebrouck, J.; Thouret, J.-C.; Hendrasto, M. Mapping the 2010 Merapi pyroclastic deposits using dual-polarization Synthetic Aperture Radar (SAR) data. *Remote Sens. Environ.* **2015**, *158*, 180–192. [CrossRef]
89. Kelfoun, K.; Legros, F.; Gourgaud, A. A statistical study of trees damaged by the 22 November 1994 eruption of Merapi volcano (Java, Indonesia): Relationships between ash-cloud surges and block-and-ash flows. *J. Volcanol. Geotherm. Res.* **2000**, *100*, 379–393. [CrossRef]
90. Pierson, T.C.; Major, J.J. Hydrogeomorphic effects of explosive volcanic eruptions on drainage basins. *Annu. Rev. Earth Planet. Sci.* **2014**, *42*, 469–507. [CrossRef]
91. Smith, G.A.; Fritz, W.J. Volcanic influences on terrestrial sedimentation. *Geology* **1989**, *17*, 375–376. [CrossRef]
92. Smith, G.A.; Lowe, D.R. Lahars: Volcano hydrologic-events and deposition in the debris flow—Hyperconcentrated flow continuum. In *Sedimentation in Volcanic Settings*; Society for Sedimentary Geology: Tulsa, OK, USA, 1991.
93. De Bélizal, E.; Lavigne, F.; Hadmoko, D.S.; Degeai, J.-P.; Dipayana, G.A.; Mutaqin, B.W.; Marfai, M.A.; Coquet, M.; Le Mauff, B.; Robin, A.-K.; et al. Rain-triggered lahars following the 2010 eruption of Merapi volcano, Indonesia: A major risk. *J. Volcanol. Geotherm. Res.* **2013**, *261*, 330–347. [CrossRef]
94. Gob, F.; Gautier, E.; Virmoux, C.; Grancher, D.; Tamisier, V.; Primanda, K.W.; Wibowo, S.B.; Sarrazin, C.; de Belizal, E.; Ville, A.; et al. River responses to the 2010 major eruption of the Merapi volcano, central Java, Indonesia. *Geomorphology* **2016**, *273*, 244–257. [CrossRef]
95. Lavigne, F.; de Bélizal, E.; Cholik, N.; Aisyah, N.; Picquout, A.; Mei, E.T.W. Lahar hazards and risks following the 2010 eruption of Merapi volcano, Indonesia. *EGU Gen Assem.* **2011**, *13*, 2011–4400.
96. Lavigne, F.; Thouret, J.C.; Voight, B.; Suwa, H.; Sumaryono, A. Lahars at Merapi volcano, Central Java: An overview. *J. Volcanol. Geotherm. Res.* **2000**, *100*, 423–456. [CrossRef]
97. Lavigne, F.; Thouret, J.-C. Sediment transportation and deposition by rain-triggered lahars at Merapi Volcano, Central Java, Indonesia. *Geomorphology* **2003**, *49*, 45–69. [CrossRef]

98. Damby, D.E.; Horwell, C.J.; Baxter, P.J.; Delmelle, P.; Donaldson, K.; Dunster, C.; Fubini, B.; Murphy, F.A.; Nattrass, C.; Sweeney, S.; et al. The respiratory health hazard of tephra from the 2010 Centennial eruption of Merapi with implications for occupational mining of deposits. *J. Volcanol. Geotherm. Res.* **2013**, *261*, 376–387. [CrossRef]
99. Lavigne, F.; Thouret, J.-C.; Hadmoko, D.S.; Sukatja, B. Lahars in Java: Initiations, dynamics, hazard assessment and deposition processes. *Forum Geogr.* **2007**, *21*. [CrossRef]
100. Saepuloh, A.; Urai, M.; Aisyah, N.; Widiwijayanti, C.; Jousset, P. Interpretation of ground surface changes prior to the 2010 large eruption of Merapi volcano using ALOS/PALSAR, ASTER TIR and gas emission data. *J. Volcanol. Geotherm. Res.* **2013**, *261*, 130–143. [CrossRef]
101. BNPB Peta Kawasan Rawan Bencana Gunung Merapi. Available online: http://www.webcitation.org/6pimWt1Fc (accessed on 20 March 2018).
102. BNPB Peta Kawasan Rawan Bencana Merapi. Available online: http://geospasial.bnpb.go.id/wp-content/uploads/2011/05/2011-04-29_KRB_Area_Terdampak_Langsung_Merapi.pdf (accessed on 9 October 2015).
103. Minnesota Population Center. *Integrated Public Use Microdata Series, International*, version 6.4; University of Minnesota: Minneapolis, MN, USA, 2015.
104. BNPB Peta Lokasi dan Jumlah Pengungsi Letusan G.Api Merapi di Wilayah Kab. Sleman (15 nov). Available online: http://www.webcitation.org/6piPoQCLs (accessed on 14 April 2017).
105. BNPB Peta Lokasi dan Jumlah Pengungsi Letusan G.Api Merapi di Wilayah Kab. Bantul (11 nov). Available online: http://www.webcitation.org/6pikQru7D (accessed on 14 April 2017).
106. BNPB Peta Lokasi dan Jumlah Pengungsi Letusan G.Api Merapi di Wilayah Kota Yogyakarta (15 nov). Available online: http://www.webcitation.org/6pilvuYiE (accessed on 14 April 2017).
107. BNPB Peta Lokasi dan Jumlah Pengungsi Letusan G.Api Merapi di Wilayah Kab. Kulon Progo (15 nov). Available online: http://www.webcitation.org/6piskXxQF (accessed on 14 April 2017).
108. Budiyono, A.F. Informasi Posko Pengungsian Merapi DIY (Update 10 November 2010). Available online: http://www.webcitation.org/6pWJmis9R (accessed on 6 April 2017).
109. GEOFABRIK Download OpenStreetMap Data for This Region: Indonesia. Available online: http://www.webcitation.org/6t07rwZox (accessed on 26 August 2017).
110. Slemankab Update Data Korban Bencana Erupsi Gunung Merapi. 2010. Available online: http://www.webcitation.org/6xi7fofUK (accessed on 6 March 2018).
111. Jumadi; Carver, S.; Quincey, D. ABM and GIS-based multi-scenarios volcanic evacuation modelling of Merapi. *AIP Conf. Proc.* **2016**, *1730*, 050005.
112. Borshchev, A. *The Big Book of Simulation Modeling: Multimethod Modeling with AnyLogic 6*; AnyLogic North America: Lebanon, NJ, USA, 2013.
113. Muhammad, A. Kemenhub Sosialisasikan Batas Kecepatan Kendaraan Di Jalan Raya. Available online: http://www.webcitation.org/6tWdf8s7A (accessed on 16 September 2017).
114. Mei, E.T.W.; Lavigne, F. Mass evacuation of the 2010 Merapi eruption. *Int. J. Emerg. Manag.* **2013**, *9*, 298–311. [CrossRef]
115. Anderson, W.A. Disaster Warning and Communication Processes in Two Communities. *J. Commun.* **1969**, *19*, 92–104. [CrossRef] [PubMed]
116. Durage, S.W.; Wirasinghe, S.C.; Ruwanpura, J.Y. Decision Analysis for Tornado Warning and Evacuation. *Nat. Hazards Rev.* **2016**, *17*, 04015014. [CrossRef]
117. Thompson, R.R.; Garfin, D.R.; Silver, R.C. Evacuation from Natural Disasters: A Systematic Review of the Literature. *Risk Anal.* **2017**. [CrossRef] [PubMed]
118. Kennedy, W.G. Modelling human behaviour in agent-based models. In *Agent-Based Models of Geographical Systems*; Springer: Berlin, Germany, 2012; pp. 167–179.
119. Robinson, E.J.H.; Franks, N.R.; Ellis, S.; Okuda, S.; Marshall, J.A.R. A Simple Threshold Rule Is Sufficient to Explain Sophisticated Collective Decision-Making. *PLoS ONE* **2011**, *6*, e19981. [CrossRef] [PubMed]
120. Huang, Z.; Williamson, P. *A Comparison of Synthetic Reconstruction and Combinatorial Optimisation Approaches to the Creation of Small-Area Microdata*; Department of Geography, University of Liverpool: Liverpool, UK, 2001.
121. Van Dam, K.H.; Bustos-Turu, G.; Shah, N. A methodology for simulating synthetic populations for the analysis of socio-technical infrastructures. In *Advances in Social Simulation 2015*; Springer: Berlin, Germany, 2017; pp. 429–434.

122. Heppenstall, A.J.; Harland, K.; Smith, D.M.; Birkin, M.H. Creating realistic synthetic populations at varying spatial scales: A comparative critique of population synthesis techniques. In Proceedings of the Geocomputation 2011 Conference, London, UK, 20–22 July 2011; pp. 1–8.
123. Harland, K.; Heppenstall, A.; Smith, D.; Birkin, M. Creating realistic synthetic populations at varying spatial scales: A comparative critique of population synthesis techniques. *J. Artif. Soc. Soc. Simul.* **2012**, *15*, 1–15. [CrossRef]
124. Moeckel, R.; Spiekermann, K.; Wegener, M. Creating a synthetic population. In Proceedings of the 8th International Conference on Computers in Urban Planning and Urban Management (CUPUM), Sendai, Japan, 27–29 May 2003; pp. 1–18.
125. BPS Sleman Dalam Angka. 2011. Available online: http://www.webcitation.org/6tTCrkUPU (accessed on 14 September 2017).
126. Adiga, A.; Beckman, R.; Bisset, K.; Chen, J.; Chungbaek, Y.; Eubank, S.; Marathe, H.S.; Nordberg, E.; Rivers, C.; Stretz, P.; et al. Synthetic populations for epidemic modeling. In Proceedings of the International Conference on Computation and Social Sciences (ICCSS), Helsinki, Finland, 8–11 June 2015.
127. Wise, S. Using Social Media Content to Inform Agent-Based Models for Humanitarian Crisis Response. Ph.D. Thesis, George Mason University, Fairfax, VA, USA, 2014.
128. Troitzsch, K.G. Validating simulation models. In Proceedings of the 18th European Simulation Multiconference, Magdeburg, Germany, 13–16 June 2004; pp. 98–106.
129. Local Government of Sleman Pemerintah Kabupaten Sleman Update Data Pengungsi Bencana Merapi 2010. Available online: http://www.webcitation.org/6pNWR8K4a (accessed on 31 March 2017).
130. Hagen-Zanker, A. Comparing Continuous Valued Raster Data: A Cross Disciplinary Literature Scan. Available online: http://epubs.surrey.ac.uk/790371/ (accessed on 24 January 2018).
131. Visser, H.; Nijs, T. The Map Comparison Kit. *Environ. Model. Softw.* **2006**, 346–358. [CrossRef]
132. Bigiarini, M.Z. Root Mean Square Error. Available online: http://www.webcitation.org/6x2E7KY2O (accessed on 5 February 2018).
133. Crooks, A.; Heppenstall, A.; Malleson, N. Agent-based modeling. In *Comprehensive Geographic Information Systems*; Elsevier: Oxford, UK, 2018.
134. Ghasemi, A.; Zahediasl, S. Normality Tests for Statistical Analysis: A Guide for Non-Statisticians. *Int. J. Endocrinol. Metab.* **2012**, *10*, 486–489. [CrossRef] [PubMed]
135. Haneberg, W. *Computational Geosciences with Mathematica*; Springer Science & Business Media: Berlin, Germany, 2004; ISBN 978-3-540-40245-9.
136. Adam, C.; Gaudou, B. Modelling Human Behaviours in Disasters from Interviews: Application to Melbourne Bushfires. *J. Artif. Soc. Soc. Simul.* **2017**, *20*, 12. [CrossRef]
137. Hagen, A. Fuzzy set approach to assessing similarity of categorical maps. *Int. J. Geogr. Inf. Sci.* **2003**, *17*, 235–249. [CrossRef]
138. Hagen-Zanker, A.; Straatman, B.; Uljee, I. Further developments of a fuzzy set map comparison approach. *Int. J. Geogr. Inf. Sci.* **2005**, *19*, 769–785. [CrossRef]
139. Briggs, W.M.; Levine, R.A. Wavelets and Field Forecast Verification. *Mon. Weather Rev.* **1997**, *125*, 1329–1341. [CrossRef]
140. Rai, V.; Robinson, S.A. Agent-based modeling of energy technology adoption: Empirical integration of social, behavioral, economic, and environmental factors. *Environ. Model. Softw.* **2015**, *70*, 163–177. [CrossRef]
141. Crooks, A.T.; Hailegiorgis, A.B. An agent-based modeling approach applied to the spread of cholera. *Environ. Model. Softw.* **2014**, *62*, 164–177. [CrossRef]
142. Tobin, G.A.; Whiteford, L.M. Community Resilience and Volcano Hazard: The Eruption of Tungurahua and Evacuation of the Faldas in Ecuador. *Disasters* **2002**, *26*, 28–48. [CrossRef] [PubMed]
143. Elder, K.; Xirasagar, S.; Miller, N.; Bowen, S.A.; Glover, S.; Piper, C. African Americans' Decisions Not to Evacuate New Orleans Before Hurricane Katrina: A Qualitative Study. *Am. J. Public Health* **2007**, *97*, S124–S129. [CrossRef] [PubMed]
144. Riad, J.K.; Norris, F.H.; Ruback, R.B. Predicting Evacuation in Two Major Disasters: Risk Perception, Social Influence, and Access to Resources. *J. Appl. Soc. Psychol.* **1999**, *29*, 918–934. [CrossRef]
145. Joglosemar Pengungsi Meningkat 10 Kali Lipat. Available online: http://www.webcitation.org/6plZ8aDi7 (accessed on 16 April 2017).

146. JPNN Pengungsi Merapi Lari Ke Gunungkidul. Available online: http://www.webcitation.org/6plXZgtDJ (accessed on 16 April 2017).
147. Ramdan, D.M. Pengungsi Sudah Masuk Bantul Sampai Gunung Kidul. Available online: http://www.webcitation.org/6plYQ7im5 (accessed on 16 April 2017).
148. Cheng, G.; Wilmot, C.G.; Baker, E.J. A destination choice model for hurricane evacuation. In Proceedings of the 87th Annual Meeting Transportation Research Board, Washington, DC, USA, 13–17 January 2008; pp. 13–17.